CO_2 REUSE IN PETROCHEMICAL FACILITIES

Phase I Final Report

Reporting Period:
January 15, 2010 to December 31, 2010

By

Jason P. Trembly, Brian S. Turk, Maruthi Pavani, Jon McCarty, Chris Boggs,
Aqil Jamal, and Raghubir P. Gupta

DOE Cooperative Agreement No. DE-FE0002147

Submitted by:

RTI International
P.O. 12194
Research Triangle Park, NC 27709-2194

April 2011

RTI INTERNATIONAL

Disclaimer

Acknowledgements

This project was sponsored by the National Energy Technology Laboratory (NETL) of the U.S. Department of Energy (DOE) under Contract No. DE-FE0002147. This financial assistance from DOE/NETL is gratefully acknowledged. In addition, the major cost-sharing for this project was provided by Kellogg, Brown and Root (KBR), Süd-Chemie (SCI), and RTI. Recognition of contributing individuals from these organizations is provided below.

DOE/NETL: Elaine Everitt, Daniel Driscoll, and Daniel Cicero.

KBR: Hugh Brian and John Super.

Süd-Chemie: Troy Walsh, Tom Pusty, and Jeff Braden.

RTI: Engineering and Analytical Support: Gary Howe, Stephen Reynolds, and Wesley Yellin. Technical Support: Ernie Johnson. Financial Support: Evan Picard. Administrative Support: Deanna Penick.

Table of Contents

Section **Page**

List of Tables

Number **Page**

List of Figures

Number **Page**

Abstract

To address public concerns regarding the consequences of climate change from anthropogenic carbon dioxide (CO_2) emissions, the U.S. Department of Energy's National Energy Technology Laboratory (DOE/NETL) is actively funding a CO_2 management program to develop technologies capable of mitigating CO_2 emissions from power plant and industrial facilities. Over the past decade, this program has focused on reducing the costs of carbon capture and storage technologies. Recently, DOE/NETL launched an alternative CO_2 mitigation program focused on beneficial CO_2 reuse to support the development of technologies that mitigate emissions by converting CO_2 into valuable chemicals and fuels.

RTI, with DOE/NETL support, has been developing an innovative beneficial CO_2 reuse process for converting CO_2 into substitute natural gas (SNG) by using by-product hydrogen (H_2)-containing fuel gas from petrochemical facilities. This process leveraged commercial reactor technology currently used in fluid catalytic crackers in petroleum refining and a novel nickel (Ni)-based catalyst developed by RTI. The goal was to generate an SNG product that meets the pipeline specifications for natural gas, making the SNG product completely compatible with the existing natural gas infrastructure. RTI's technology development efforts focused on demonstrating the technical feasibility of this novel CO_2 reuse process and obtaining the necessary engineering information to design a pilot demonstration unit for converting about 4 tons per day (tons/day) of CO_2 into SNG at a suitable host site.

This final report describes the results of the Phase I catalyst and process development efforts. The methanation activity of several commercial fixed-bed catalysts was evaluated under fluidized-bed conditions in a bench-scale reactor to identify catalyst performance targets. RTI developed two fluidizable Ni-based catalyst formulations (Cat-1 and Cat-3) that demonstrated equal or better performance than that of commercial methanation catalysts. The Cat-1 and Cat-3 formulations were successfully scaled up using commercial manufacturing equipment at the Süd-Chemie Inc. pilot-plant facility in Louisville, KY. Pilot transport reactor testing with RTI's Cat-1 formulation at Kellog Brown & Root's Technology Center demonstrated the ability of the process to achieve high single-pass CO_2 conversion. Using information acquired from bench- and pilot-scale testing, a basic engineering design package was prepared for a 4-ton/day CO_2 pilot demonstration unit, including process and instrumentation diagrams, equipment list, control philosophy, and preliminary cost estimate.

Executive Summary

The objective of this project was the development of a novel transport reactor-based methanation technology capable of converting carbon dioxide (CO_2) into pipeline-quality substitute natural gas (SNG) by using by-product hydrogen (H_2)-containing fuel gas from petrochemical facilities. This process represents an attractive means to use and reuse CO_2 to produce SNG that can be used in the existing natural-gas infrastructure. Information obtained during the research and evaluation phase of this project clearly demonstrated that this process is both technically and economically feasible and warrants development to a larger scale.

The process technology developed in this project leveraged commercial reactor designs currently used in the petroleum refining industry (fluid catalytic crackers) and a novel, fluidizable nickel (Ni)-based catalyst developed by RTI International (RTI) [1]. In this process, RTI's catalyst was circulated through a transport reactor where it came into contact with CO_2 and H_2 and catalyzed the conversion of these reagents into pipeline-quality SNG. Integrating the transport reactor with a fluidizable Ni-based catalyst represented an advancement over commercial methanation systems, which typically suffer from poor thermal management and large size. During methanation of CO_2 and H_2, heat is released and, if not properly controlled, can adversely affect catalyst performance. In RTI's process, the transport reactor design allowed for high throughput (because of high gas velocities) and significantly improved temperature control. The catalyst acted as a heat sink for the exothermic methanation reaction and was then circulated into a solids cooler, where indirect contact with cooling water removed the heat through production of high-pressure steam. This approach limited the temperature rise across the reactor and allowed for high single-pass CO_2 conversion and a much smaller reactor footprint compared to that of commercial methanation systems.

Development of RTI's novel CO_2 reuse process was based on a two-phase approach. Phase I activities were focused on catalyst and process development activities, including optimization and scale-up of RTI's fluidizable Ni-based catalyst, evaluation testing in a pilot-plant transport reactor, techno-economic analyses, and development of a basic engineering design (BED) package for potential field demonstration in Phase II. Phase II activities would include the design, construction, and demonstration of a pilot-scale transport reactor–based methanation system. The proposed pilot unit would convert 4 tons per day (tons/day) of CO_2 and provide the operational and engineering information needed to validate the commercial viability of this technology.

In Phase I of this project, significant progress was made in developing a truly novel fluidizable methanation catalyst. RTI relied heavily on our expertise gained from more than 20 years of catalysis work on fluidized and transport reactor applications to develop new synthesis procedures for the Ni-based

[1] RTI International is a trade name of Research Triangle Institute.

methanation catalyst for this project. In addition, an existing bench-scale test unit was extensively used to conduct benchmarking experiments of commercial fixed-bed catalysts. The benchmarking data were used to develop performance targets for the fluidizable catalysts and help with optimization of catalyst properties. Through a series of parametric evaluations, RTI optimized the synthesis procedures for two fluidizable Ni catalyst formulations (Cat-1 and Cat-3) that possessed equal or better methanation activity compared to that of commercial fixed-bed catalyst formulations. RTI's catalysts have demonstrated up to 3.5 times greater methanation activity at 200 °C. Following bench-scale development, RTI and Süd-Chemie, Inc. (SCI) worked together to produce a 100-lb batch each of the Cat-1 and Cat-3 formulations using commercial manufacturing equipment at SCI's pilot-plant facility in Louisville, KY. The methanation activity exhibited by the commercially prepared RTI Cat-1 catalyst was similar to that of the laboratory-prepared material.

The commercially prepared Cat-1 catalyst was tested at KBR's (formerly known as Kellogg Brown & Root) transport reactor test facility in Houston, TX. In parallel, to further evaluate transport reactor operation, a computational fluid dynamics (CFD) model was developed using the bench- and pilot-scale data collected. The results from both pilot-scale transport reactor and CFD model demonstrated the ability of the transport reactor to achieve high single-pass CO_2 conversions, while limiting temperature rise to 45 °C. RTI used testing and modeling data to develop a BED package for a 4-ton/day CO_2 pilot demonstration unit. This comprehensive BED package included a process flow diagram, process and instrumentation diagrams, plot plans, an interface diagram, an equipment list, control philosophy, and a preliminary cost estimate. In addition, the techno-economic evaluation was further updated using pilot-plant results. This updated analysis confirmed the economic advantages of RTI's novel CO_2 reuse process over conventional methanation technologies for CO_2 conversion.

1. Introduction

Anthropogenic sources of carbon dioxide (CO_2) have become a major public concern in recent years due to the consequences of climate change from increasing atmospheric CO_2 concentrations. The U.S. government has recently begun to position itself to regulate CO_2 emissions under the U.S. Clean Air Act by declaring CO_2 a danger to public welfare. In addition, President Barak Obama's administration has begun to develop a global climate change strategy to limit temperature rise to 2 °C by 2050. Carbon capture and storage (CCS) technology represents a practical solution for controlling CO_2 emissions; therefore, the U.S. Department of Energy is actively funding projects for commercial deployment of CCS technology in the near future. Alternatively, CO_2 reuse technologies can also mitigate emissions by converting CO_2 into valuable chemicals and fuels rather than using geologic storage.

The key technical challenge associated with reuse technologies is the stability of CO_2. As the most fully oxidized form of carbon, CO_2 has the lowest energy content and is extremely chemically stable. Converting CO_2 into more desirable chemicals and fuels therefore requires the addition of energy to the CO_2 molecule. The most desirable reactant for the conversion of CO_2 into fuels and/or chemicals is H_2. The problem is that H_2 must be produced from less energetic reactants that occur naturally, such as methane and water. Because methane is carbon-based, its use for H_2 production for CO_2 reuse is not practical. The cleavage of water to produce H_2 does have more potential, provided the energy is not derived from the oxidation of carbon fossil fuels. Energy sources that meet this requirement include nuclear and renewable, primarily solar and wind.

Nuclear-based H_2 production is commercially practical because it combines two industrially proven technologies, nuclear power production and water electrolysis. However, because the U.S. has not built a new nuclear power plant since 1977 and public support for nuclear technology is extremely low, large-scale nuclear-based H_2 will not be available in the near future (25-50 years). Although solar-based H_2 production technology is based on renewable solar energy and enjoys strong public support, the costs associated with making H_2 with solar energy are currently not economical and will remain so for the near term. Wind-based power production, which is more economical, has seen significant growth over recent years, but its limited projected capacity through 2030 will be insufficient to make any appreciable impact on CO_2 emissions.

Another potential source of H_2 is a chemical process that produces a primary product accompanied by the generation of H_2 as a secondary by-product. Because this process has a fixed CO_2 footprint for a specific production rate and produces multiple products beyond the primary product, the net CO_2 footprint for each product is smaller. Under these circumstances, the use of the H_2 by-product for CO_2 reuse would result in a net reduction of CO_2 emissions and CO_2 footprint for the process.

One chemical process that fits this description is ethylene production. Ethylene is produced during steam cracking of ethane, propane, and/or naphtha. Because this reactive process targets the removal of H_2 from the hydrocarbon molecules to create olefins, in particular ethylene, and aromatics, H_2 and methane are also produced as by-products. Because ethylene is a large-scale, commodity chemical with net annual global demand of 140 million tons in 2010 and a U.S. production capacity representing 28% of this total, a significant amount of H_2 is available at ethylene plants in the U.S [2]. This H_2 is separated with methane to create a fuel-gas by-product. Some of this fuel gas is used to provide the heat required to drive the endothermic cracking reactions and other process energy requirements. However, a significant portion of the fuel gas is merely used for its heat content. Therefore, the H_2 by-product produced at ethylene plants represents a unique opportunity and starting point for implementing CO_2 reuse technologies in the near future.

[2] K.R. Hall, Catal. Today, 106, 243 (2005).

2. Background

2.1 Theory

RTI has been working on the development of a reuse technology that converts CO_2 into pipeline-quality SNG by using H_2 by-product from ethylene production facilities. The chemistry for this reuse process is based on the Sabatier reaction shown in Equation 1:

$$CO_2 + 4H_2 = CH_4 + 2H_2O,\ \Delta H = -165\ \text{kJ/mol} \quad [1]$$

RTI's novel process, shown in Figure 2-1, uses a transport reactor methanator (TRM) equipped with a solids cooler and an attrition-resistant nickel (Ni)-based catalyst. There are many advantages to using this process approach. For instance, the process

- Upgrades the fuel-gas mixture available in ethylene plants to pipeline-quality SNG
- Intensifies process configuration by using a single reactor to achieve high conversion and throughput
- Effectively uses a transport reactor to minimize process footprint
- Effectively controls reactor temperature for the highly exothermic reaction by using the circulating solid catalyst to absorb the heat and a solids cooler to extract the heat from the circulating solids
- Extracts the heat from the exothermic reaction as high-pressure, saturated steam
- Minimizes additional processing of the feed and product streams

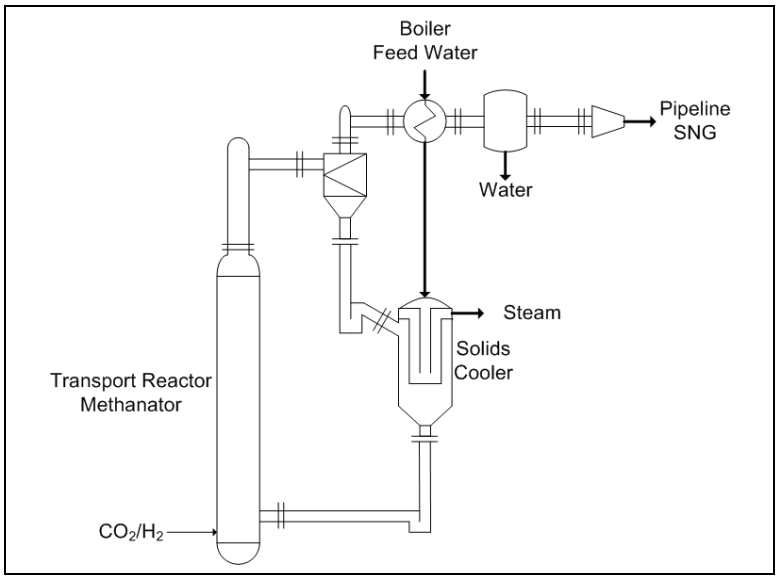

Figure 2-1. Schematic of RTI's TRM process.

In the TRM process, the fuel gas and CO_2 are introduced into the bottom of the transport reactor. The flow of these gases entrains the solid catalyst through the transport reactor. The entrainment of the solids by the reaction gas promotes excellent mixing of the catalyst and reactants, ensuring optimal mass and heat transfer. Because of this excellent mass transfer, the catalyst rapidly catalyzes the Sabatier reaction, resulting in the conversion of CO_2 into SNG. In addition, the solid catalyst particles absorb the heat of the reaction effectively, moderating the heat released by the exothermic reaction. At the top of the transport reactor, the hot solid catalyst particles and gas products are separated by a cyclone. This cyclone feeds the

hot catalyst particles into a solids cooler, which is used to generate high-pressure, saturated steam. The cooled catalyst particles are then returned to the bottom of the transport reactor and recycled back to the riser for methanation of CO_2.

Minimal additional processing of the product SNG gas would be required to meet natural-gas pipeline specifications. These processing steps would most likely include cooling, separation of the water (H_2O) byproduct, and compression. Additional processing steps might include more filtration to remove fine particulate matter and an additional treatment to adjust H_2 and CO_2 content of the SNG product to meet pipeline specifications.

2.2 Competing Technologies

Conventional commercial methanation processes use fixed-bed reactors filled with a Ni-based catalyst. The primary applications of these methanation systems are in ammonia (NH_3) plants and for SNG production from synthesis gas. In NH_3 synthesis, catalysts are poisoned by carbon monoxide (CO) and CO_2, making the removal of CO and CO_2 from the feed stream to the NH_3 reactor imperative. Methanation represents the final step in this removal process, effectively converting the typical 0.1–0.3 volume percent (vol%) of CO and CO_2 into CH_4, which acts as an inert in the NH_3 reactor. Due to the upstream processing, which includes water-gas-shift reactors and a CO_2 separation process, the CO_2 concentration is significantly higher than that of CO in the feed stream to the methanator. This fact demonstrates that the commercial Ni-based methanation catalyst effectively converts not only CO but also CO_2 into CH_4 and can perform this conversion in a gas mixture of CO and CO_2.

Because of the very low CO and CO_2 concentrations in the methanator feed in an NH_3 plant, no special reactor design features are required for temperature control resulting from the exothermic methanation reaction. However, this is not the case for synthesis gas conversion into SNG, in which the temperature rise across the reactor for every mole percent of carbon oxide species reacted is 50–74 °C for CO and 40–60 °C for CO_2. Two distinct processes are typically used to achieve temperature control for methanation of synthesis gas (Figure 2-2). One process incorporates a large product recycle to control methanator temperature; the other process uses interstage cooling with multiple methanation reactors in a once-through process.

Examination of the process flow diagrams (PFDs) in Figure 2-2 shows that both conventional approaches for temperature control require multiple reactors and heat exchangers. Both processes also use an inert diluent to decrease the reactant concentrations, effectively lowering the per-pass conversion in the reactor and providing an additional means of removing the reaction heat as sensible heat.

In our process, there is a single transport reactor and solids cooler. Thus, a significant amount of equipment and operating complexity is removed compared to conventional methanation systems. The circulating solid catalyst is used to remove reaction heat out of the reactor as sensible heat. This process offers the following two distinct advantages:

- Because reactor systems are fixed-volume systems and solids are denser than gases, more mass of solids can be moved through a reactor system than gas. As a result, the moving solids can remove significantly more reaction heat as sensible heat in a transport reactor.
- For the same amount of reaction heat, the temperature rise in the solids will be much smaller because of its larger mass. This significantly increases the amount of per-pass conversion that can be accommodated in the transport reactor while maintaining reactor temperature below temperatures that would result in catalyst sintering and/or weakening of the reactor vessels. This means multiple reactors and diluents are not necessary to limit per-pass conversion in a transport reactor system. This effect can also be used to operate the transport reactor system within a narrower temperature window and at lower temperatures that favor higher equilibrium conversion to CH_4.

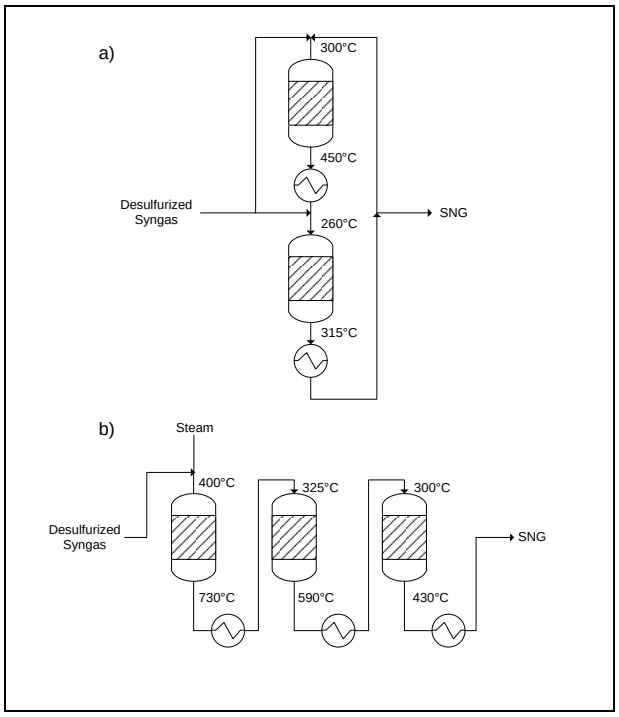

Figure 2-2. Methanator reactor systems: (a) Lurgi SNG process and (b) ICI SNG process [3].

The final temperature control step in our process is the use of the solids cooler to remove the sensible heat from the solids. Although heat transfer coefficients between fluids and a solid wall in the typical heat exchanger are relatively low [approximately 20 Btu/(h·ft^2·°F) for gases and 35 Btu/(h·ft^2·°F) for liquids], the fact that the catalysts particles are small (approximately 80–100 microns [µm]) and fluidized significantly increases their heat transfer coefficient. With these high heat-transfer coefficients, moving the sensible heat out of the circulating solid catalyst should be relatively fast and effective. The solids cooler also ensures optimal transfer of this heat to produce high-pressure steam by maintaining nucleate boiling conditions. Solids coolers are currently used in commercial fluid catalytic cracking (FCC) units. These solids coolers are used extensively to effectively remove additional heat generated during combustion of coke on the FCC catalyst with O_2-enriched air.

[3] Twigg, M.V. (Editor). 1997. *Catalyst Handbook* (2nd edition). Manson Publishing.

2.3 Preliminary TRM Process Economics

Using publicly available information, an analysis of ethylene production in the United States was completed [4,5,6]. Based on this analysis, the capacity of the average ethylene plant was 1,500 million pounds per year (MMlb/yr) of ethylene. Furthermore, this analysis indicated that the H_2, along with CH_4, was separated from the demethanizer as a H_2-rich fuel gas by-product. Estimates of the heat required to drive the endothermic cracking reactions and power the downstream separation equipment were used to calculate the amount of fuel gas consumed within the ethylene plant. The residual fuel gas was assumed to be excess. Table 2-1 summarizes these different estimates for ethylene plants using ethane, propane, and naphtha feedstocks. The values in Table 2-1 show that a significant amount of excess H_2-rich fuel gas is available within ethylene plants, confirming that RTI's technology for CO_2 conversion could be applied commercially at ethylene plants in the near future.

Table 2-1. Estimation of Availability of Hydrogen-Rich Fuel Gas for RTI's TRM Process in an Average Ethylene Plant[a]

Feedstock	Annual Production from an Average Ethylene Plant[a]			Fuel Gas for Process Energy Demands[b] (%)	Residual Fuel Gas	
	Ethylene (MMlb/yr)	Fuel Gas				
		H_2 (MMlb/yr)	CH_4 (MMlb/yr)		H_2 (MMlb/yr)	CH_4 (MMlb/yr)
Ethane	1,500	114	103	54.4	52	47
Propane	1,500	70	961	22.7	54	743
Naphtha	1,500	52	822	25.3	39	614

[a] The average ethylene plant was assumed to produce 1,500 MMlbs/yr of ethylene.

[b] The energy demands for RTI's TRM process include endothermic reforming heat and energy demands of downstream separations.

Using the estimated values from Table 2-1 for excess H_2-rich fuel gas available in the average ethylene plant, an estimate of the net CO_2 reduction was calculated assuming the H_2 in the available excess fuel gas could be used to convert CO_2 to SNG. This net CO_2 reduction was then used to determine the potential reduction in CO_2 footprint for the average ethylene plant and the potential revenue resulting from CO_2 credits based on two projected values for CO_2 credits. These estimates, provided in Table 2-2, show that the novel TRM process can substantially reduce the plant CO_2 footprint and generate significant revenue from CO_2 credits.

Table 2-2. Estimated Ethylene Process CO_2 Footprint and Credit Revenue Generated for an Average Ethylene Plant

Feedstock	CO_2 Footprint Reduction [%]	Potential Revenue from CO_2 Credits ($ million/average ethylene plant[a])	
		$20/ton CO_2	$50/ton CO_2
Ethane	86.0	$2.9	$7.2
Propane	50.7	$3.0	$7.4
Naphtha	62.5	$2.1	$5.4

[a] Average ethylene plant size was assumed to be 1,500 MMlbs/yr of ethylene produced.

[4] R. Karimzadeh, H.R. Godini, M. Ghashghaee, Chem. Eng. Res. Des., 87, 36 (2009).
[5] O. Uemaki, K.B. Mathur, Ind. Eng. Chem, 15, 504 (1976).
[6] D. Williams, U.S. Patent 5,990,370, 1999.

Because the novel TRM process converts CO_2 to an SNG product that meets natural-gas pipeline specifications, this SNG represents a marketable product that commands a premium price. In contrast, the value of the fuel gas is essentially limited to combustion for heat generation and commands a discounted price compared to natural gas. To determine the net value generated by upgrading the fuel-gas product, the information in Table 2-1 was used to calculate the heat values in Table 2-3 for the feed and product streams. The Table 2-3 results were then used to estimate the net revenue generated by upgrading the fuel gas to SNG. The two key assumptions made were that the value of the SNG product was $4 per million British thermal units (MMBtu) and the CO_2 feed had no associated cost. The results of this analysis for a range of differential prices between the product SNG and fuel gas are presented in Figure 2-3.

Table 2-3. Net Heat Values of Reactants and Products for the Sabatier Process in an Average Ethylene Plant[a]

Feedstock	Available Fuel Gas		CO_2 Feed (MMlb)	Heat Value of Feed Gases (Trillion Btu)	Product CH_4 (MMlb)	Heat Value of Product Gas (Trillion Btu)
	H_2 (MMlb)	CH_4 (MMlb)				
Ethane	52	47	287	4.3	114	3.6
Propane	54	743	296	21.0	850	20.0
Naphtha	39	614	215	17.0	692	16.6

[a] Average ethylene plant was assumed to produce 1,500 MMlbs/yr of ethylene.

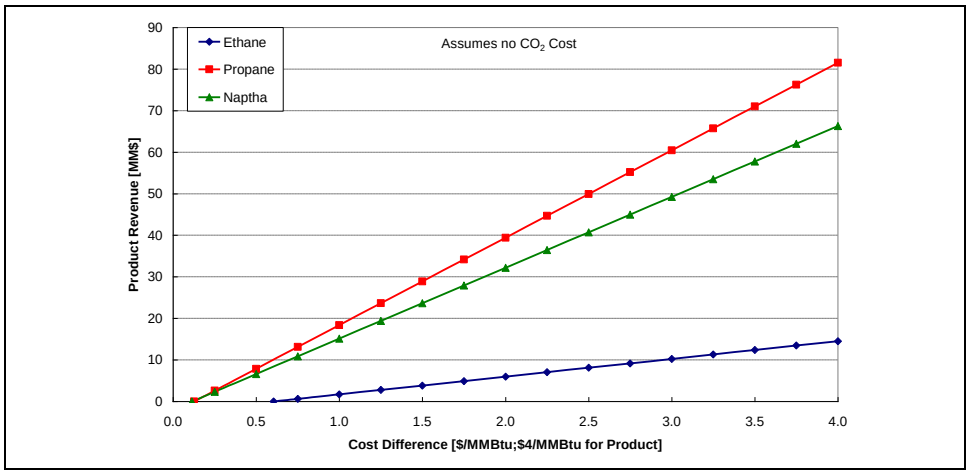

Figure 2-3. Revenue based on price differential between product SNG and fuel gas for an average ethylene plant producing 1,500 MMlb/yr of ethylene.

As shown in Figure 2-3, if the price differential between the SNG product and fuel gas is large enough, then the SNG product is more valuable than the fuel gas, and the TRM process will generate revenue. The specific price differences for which the TRM process begins to generate revenue are $0.60, $0.13, and $0.11 per MMBtu for ethane, propane, and naphtha feedstocks, respectively. Because the fuel-gas streams are a mixture of CH_4 and H_2 and no existing infrastructure exists for distributing this product to market, any consumer will demand the maximum possible price differential between fuel gas and natural gas to compensate for the inconveniences of working with the fuel gas. Thus, the differential

price is anticipated to be larger than the break-even differential prices, ensuring that RTI's TRM process will generate revenue.

The SNG product has a lower energy content than the fuel gas because the exothermic Sabatier reaction converts this energy into heat, which, in turn, is used to raise steam. Most ethylene plants have already optimized generation and use of steam from the steam-cracking process to minimize energy demands. Hence, some additional optimization effort is required to effectively use this additional steam. A potential range of values for this steam has been estimated. A lower value was estimated by assuming that this additional steam reduces the fuel costs required for steam generation. A higher value was estimated by assuming the steam is used to generate electric power, reducing the purchase of electricity for running necessary process equipment. These estimated values are provided in Table 2-4 for the different feedstocks for an average 1,500-MMlb/yr ethylene production plant.

Table 2-4. Potential Process Savings from Steam Generated by the Sabatier Process for an Average Ethylene Plant[a]

Feedstock	Steam Raised (MMlb)	CH_4 Savings[b] ($ in millions)	Electricity Savings ($ in millions)
Ethane	391	1.3	3.0
Propane	403	1.3	3.1
Naphtha	293	1.0	2.3

[a] Average ethylene plant was assumed to produce 1,500 MMlbs/yr of ethylene.
[b] Steam production costs were assumed to be $3.69 per 1,000 lbs.
[c] Electrical cost was assumed to be $0.0654 per kilowatt hour.

A preliminary techno-economic feasibility study for converting fuel gas to SNG in the average 1,500-MMlb/yr ethylene plant using ethane as the main feedstock was completed. The PFD is shown in Figure 2-4. From process material and energy balances calculated using an Aspen HYSYS model, this process would produce 10 million standard cubic feet of gas per day (MMscf/day) of pipeline-quality SNG and consume approximately 350 tons/day of CO_2 based on the available fuel gas in the plant.

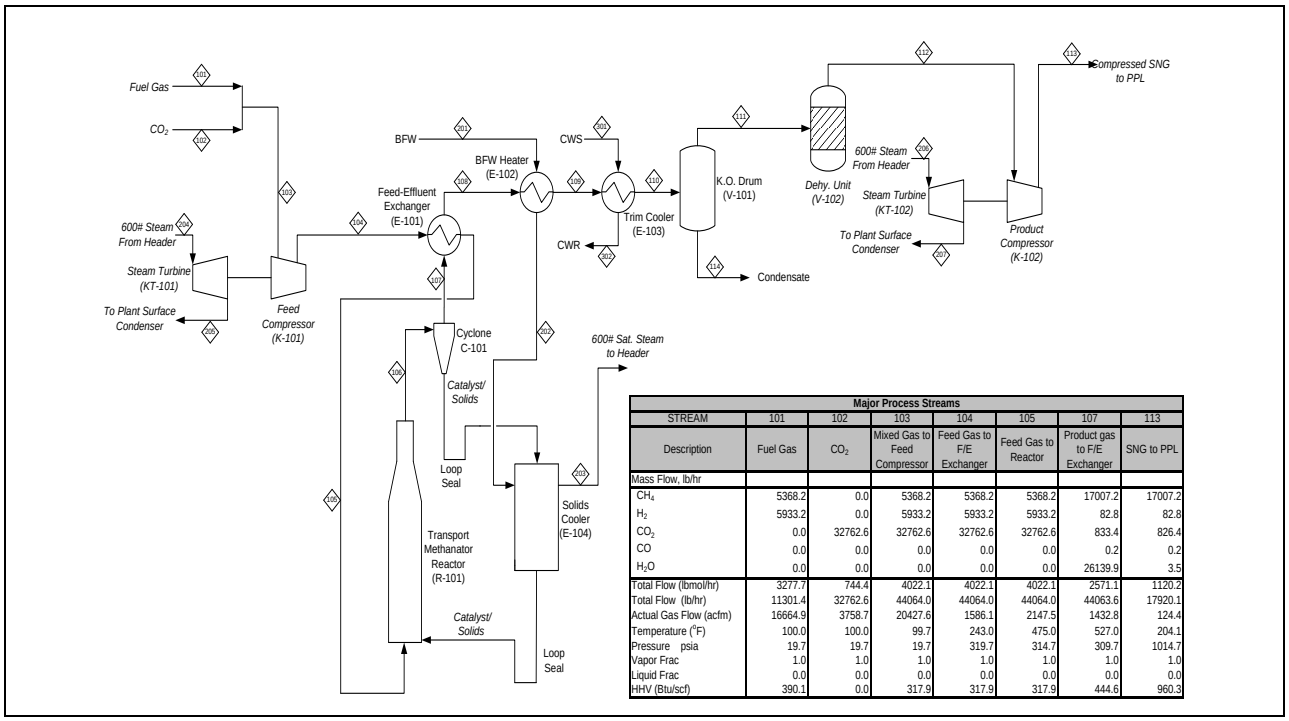

Major Process Streams							
STREAM	101	102	103	104	105	107	113
Description	Fuel Gas	CO_2	Mixed Gas to Feed Compressor	Feed Gas to F/E Exchanger	Feed Gas to Reactor	Product gas to F/E Exchanger	SNG to PPL
Mass Flow, lb/hr							
CH_4	5368.2	0.0	5368.2	5368.2	5368.2	17007.2	17007.2
H_2	5933.2	0.0	5933.2	5933.2	5933.2	82.8	82.8
CO_2	0.0	32762.6	32762.6	32762.6	32762.6	833.4	826.4
CO	0.0	0.0	0.0	0.0	0.0	0.2	0.2
H_2O	0.0	0.0	0.0	0.0	0.0	26139.9	3.5
Total Flow (lbmol/hr)	3277.7	744.4	4022.1	4022.1	4022.1	2571.1	1120.2
Total Flow (lb/hr)	11301.4	32762.6	44064.0	44064.0	44064.0	44063.6	17920.1
Actual Gas Flow (acfm)	16664.9	3758.7	20427.6	1586.1	2147.5	1432.8	124.4
Temperature (°F)	100.0	100.0	99.7	243.0	475.0	527.0	204.1
Pressure psia	19.7	19.7	19.7	319.7	314.7	309.7	1014.7
Vapor Frac	1.0	1.0	1.0	1.0	1.0	1.0	1.0
Liquid Frac	0.0	0.0	0.0	0.0	0.0	0.0	0.0
HHV (Btu/scf)	390.1	0.0	317.9	317.9	317.9	444.6	960.3

Figure 2-4. Schematic of RTI's TRM process integrated into an average 1,500-MMlb/yr ethylene plant.

The mass and energy balances were used to calculate equipment sizes and utility consumption. Table 2-5 shows the total project (or EPC) cost of the proposed facility built at an ethylene plant in the Gulf Coast region of the United States. This capital cost was based on factored estimates from previous cost data for similar equipment. Whenever necessary, the cost numbers were adjusted to August 2009 U.S. dollars by using the appropriate Chemical Engineering Index.

Table 2-5. Estimates of Capital and Production Costs

Item	Cost
Reactor system	$1,075,269
Solids cooler	$300,000
Feed effluent exchanger	$284,256
Boiler feedwater heater	$130,000
Trim cooler	$224,000
H_2O knockout drum	$60,000
Dehydration unit	$400,000
Feed compressor and turbine package	$7,873,937
Product compressor and turbine package	$2,098,480
Total process equipment cost	$12,445,941
Total field cost	$31,114,853
Subtotal professional services	$8,923,740
Subtotal owner's cost	$4,324,965
Total project (EPC) cost (±30%)	$44,363,557

Based on a total project investment of $44.4 million, a cash flow analysis was performed, and the percentage of Internal Rate of Return (IRR) was calculated for different CO_2 credit values. As shown in Table 2-6, the proposed process generated a return on investment. At a projected CO_2 credit value of ≥$20 per ton, the IRR was >19%. Hence, at CO_2 credit

Table 2-6. IRR for Different Projected CO_2 Credits

	CO_2 Credits			
	$0/ton	$10/ton	$20/ton	$30/ton
%IRR	14	17	19	22

values that match current projections, the IRR becomes large enough that commercial investment in this emerging process technology would be justified.

The net result of the preliminary techno-economic analysis is that our novel TRM process can offer significant value to an ethylene plant. This value comes from

- Net consumption of CO_2 in a beneficial reuse process
- Conversion of low-value fuel gas into premium-value SNG product
- Generation of high-pressure steam, as demonstrated in Table 2-4

The technical and financial benefits indicate that ethylene production plants represent a promising commercial application for the TRM technology. Actual commercial implementation of this process technology will be driven by the financial benefits derived from the CO_2 credits when CO_2 legislation is enacted.

3. Experimental Methods

3.1 Catalyst Synthesis

Using aqueous co-precipitation methods, RTI developed two fluidizable Ni-based catalyst formulations for CO_2 methanation. The first catalyst formulation, Cat-1, was composed of Ni supported on a nickel aluminate ($NiAl_2O_4$). The second formulation, Cat-3, consisted of Ni supported on a ceria (CeO_2)–zirconia (ZrO_2) mixed metal oxide. Both formulations were then processed as spray-dried powders for use in a transport reactor (entrained-bed) system. As discussed in Section 2, the transport reactor approach was chosen because it offers much better process heat management over fixed-bed reactor systems in that it minimizes temperature rise across the methanation reactor, while extracting the process heat of reaction in a solids cooler.

3.1.1 Co-precipitation Methods

The Cat-1 material was prepared by dissolving nickel nitrate and aluminum nitrate in deionized (DI) water to form an acidic metal salt solution. Similarly, Cat-3 was prepared by mixing nickel nitrate, zirconium oxynitrate hydrate, cerium nitrate, and DI water. Two co-precipitation methods — the constant pH method and the raised pH method — were used to form a metal hydroxide product. In the constant pH method, the metal salt solution and basic salt solution were added together simultaneously, while maintaining the pH of the continuously stirred precipitating solution between 7.0 and 9.0, depending on the choice of base. In the raised pH method, the pH of the precipitating slurry was increased from about 4.0 to 7.5 by slowly adding the basic salt solution to the acidic metal salt solution in a 5-L stirred vessel. The preparations of Cat-1 and Cat-3 were investigated using several different precipitating bases, such as ammonium hydroxide (NH_4OH), ammonium carbonate [$(NH_4)_2CO_3$], sodium hydroxide (NaOH), or sodium carbonate (Na_2CO_3). The Cat-1 material was prepared using both co-precipitation methods, and Cat-3 was prepared using only the constant pH method. While stirring, the co-precipitates were aged at room temperature for 1 h before filtering. The filtered cake was washed with DI water until the pH of the filtrate was neutral. The washed hydroxide cake was then prepared for spray drying (Section 3.1.2).

3.1.2 Spray Drying

In preparation for spray drying, the filtered and washed Cat-1 and Cat-3 catalyst cakes were mixed with a specific volume of H_2O to achieve a target solids concentration based on the percentage weight loss of the cake material (i.e., loss on ignition). The resulting slurry pH was adjusted to 4.0–5.0 using nitric acid for Cat-1 and 6.5 using acetic acid for Cat-3. When the necessary pH was achieved, the slurry was spray-dried using a Niro Mobile Minor 2000 spray dryer. Prior to introducing the slurry, the spray-dryer inlet and outlet temperatures were allowed to stabilize at 325 °C and 120 °C, respectively. The spray-dried catalyst particles were collected, dried at 120 °C for 2 h, and calcined at 300–450 °C for 4 h in ambient air.

3.2 Bench-Scale Testing

The bench-scale testing system used in the development of the fluidizable Ni-based methanation catalysts is shown in Figure 3-1. The reactor consisted of a 2-in. inside-diameter (ID) quartz tube housed in a vessel that could be pressurized at high temperatures. A bank of Brooks mass flow controllers (MFCs) was used to supply the reactor with a methanation gas mixture. The reactive gas mixture was preheated in a furnace upstream of the reactor and then passed downward through the annular space between the quartz tube and the pressure vessel wall before flowing through a quartz frit distributor and the fluidized catalyst bed. The gas exiting the reactor was cooled through a water-cooled condenser before it was sampled and analyzed by gas chromatography. A data acquisition system connected to the reactor test system was used to control experimental conditions and record data.

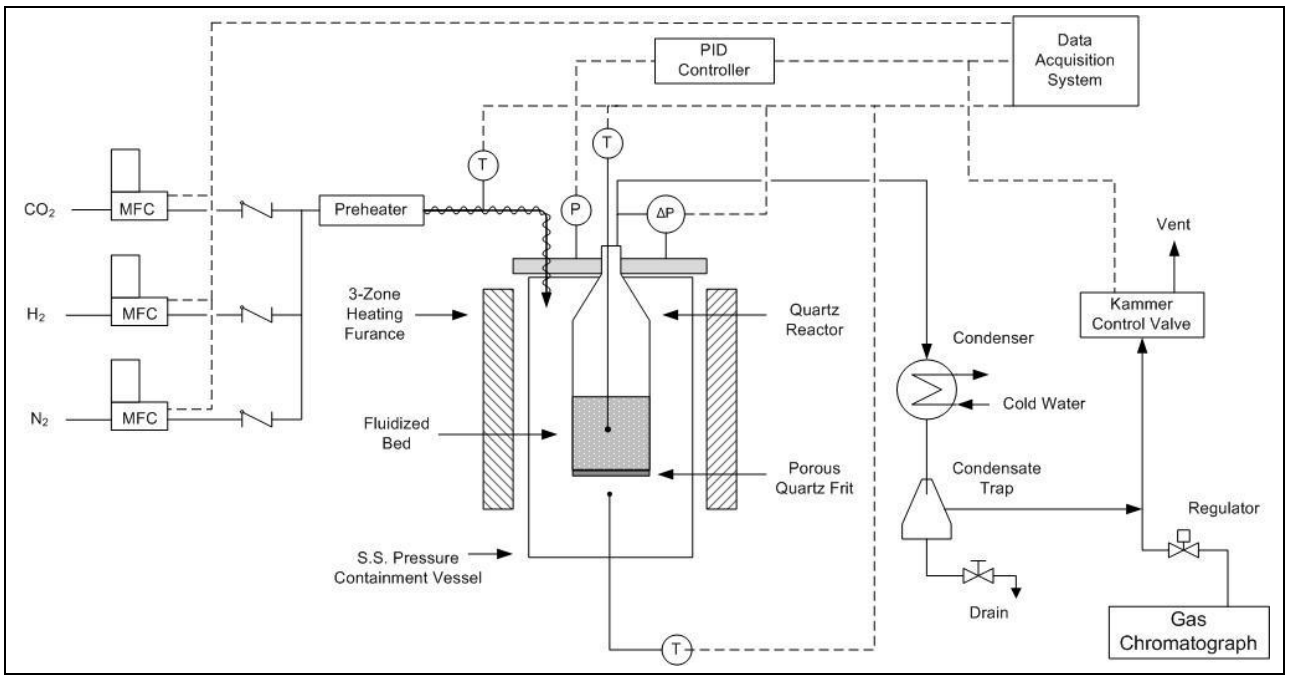

Figure 3-1. RTI's bench-scale, high-pressure catalyst testing system.

For all catalysts examined in Phase I, the same bench-scale methanation test conditions and testing protocol were used. The test conditions used are shown in Table 3-1. The catalyst bed consisted of 300 g of material comprising 25 g of active catalyst and 275 g of zinc oxide and zinc aluminate mixed oxide, which were shown to be inactive for CO_2 methanation under the test conditions. The total gas flow rate was 20 standard liters per minute (SLPM), which corresponded to a nominal gas–catalyst contact time of ~4 s for the expanded bed at 300 °C and 300 psig.

Table 3-1. Test Conditions and Gas Composition Used in Bench-Scale Tests of Methanation Catalysts

Test Conditions	
Temperature (°C)	200–350
Pressure (psig)	300
Fluidized bed	25 g catalyst / 275 g inert
Gas component	Composition (vol%)
CO_2	2.5
H_2	15.0
N_2	82.5

Note: N_2 = nitrogen; psig = pounds per square inch gauge.

To reduce the temperature rise of the exothermic methanation reaction in the bench-scale tests, a low CO_2 concentration of 2.5 vol% was used. Thermocouple probes located within the catalyst bed at 1, 3, and 5 in. from the gas distribution frit typically showed ~5 °C rise across the bed. The H_2/CO_2 feed gas ratio for the comparative methanation tests was 6.0 rather than the stoichiometric ratio of 4.0. This avoided the problem of CO_2 conversion kinetics becoming highly non-linear (as much as 5th order in reactant concentration) as the already low levels of CO_2 fell below 1 vol% and masking significant differences in relative activity of the various catalysts. Using the feed gas ratio of 6.0 in bench-scale tests, the maximum CO_2 conversion observed for highly active catalysts was typically 95% to 98%, corresponding to 0.12 to 0.05 vol% residual CO_2 in the effluent gas, respectively, while H_2 levels approached 5 vol%. Tests with selected catalysts using stoichiometric gas ratios (3.0 vol% CO_2 and 12.0 vol% H_2) showed similar conversion rates at low temperature, but, as the CO_2 conversion increased beyond 50%, these rates slowed appreciably. An investigation of the detailed reaction kinetics for CO_2 methanation approaching equilibrium values with near stoichiometric feed ratios was beyond the scope of this Phase I project, but it will need to be performed as part of the continued development of the TRM process.

4. Results and Discussion

4.1 Bench-Scale Fluidized-Bed Testing of Methanation Catalysts

4.1.1 Commercial Methanation Catalyst Screening

To establish performance targets for fluidized-catalyst development, initial bench-scale testing was conducted with commercial methanation catalysts as reference materials. Because a key innovation of RTI's novel CO_2 reuse process is the use of a transport reactor and all commercial methanation catalysts are in the form of tablets or extruded pellets, it was necessary in this project to process these materials to give them better fluidization characteristics for the transport reactor process.

Five commercial Ni-based methanation catalysts, identified as Com-A, Com-B, Com-C, Com-D, and Com-E, were obtained, crushed, and sieved to particle sizes ranging from 75 to 120 μm and evaluated in RTI's bench-scale reactor system (Figure 3-1). The standard catalyst activation procedure for these fluidized tests was reduction at 350 °C under H_2 partial pressure of 38 psia. The experimental process conditions summarized previously in Table 3-1 were used in these bench-scale studies. The CO_2 methanation performance of these fluidized commercial catalyst samples are shown in Figure 4-1. The commercial methanation catalysts demonstrated high activity and nearly 100% selectivity for CH_4. Most of these reference catalysts became active, showing significant conversion of CO_2, at temperatures between 175 and 250 °C. The more active commercial catalysts set very high performance targets for the development of RTI's fluidizable catalysts.

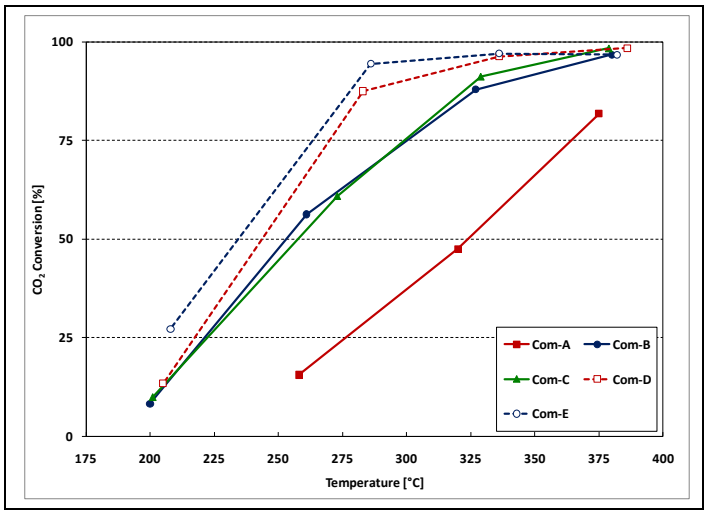

Figure 4-1. CO_2 methanation activity measured on reference commercial methanation catalysts.

The attrition resistance of these processed commercial catalysts was measured using a modified Davison jet-cup method in which a 5-g catalyst powder sample was entrained, collected, and recirculated in an air jet that impinged onto a thimble for 30 min. The attrition index and other properties of the crushed commercial methanation catalysts are presented in Table 4-1. Attrition resistance is an important selection criterion for fluidizable catalysts because it ensures that sufficient catalyst remains in the pilot-plant reactor to complete testing and provide sufficient data for process development.

Table 4-1. Commercial Methanation Catalyst Properties

Catalyst	Commercial Form	Powder Density (g/cm^3)	Davison Index[a]
Com-A	Pellet	1.2	40.7
Com-B	Pellet	1.4	12.3
Com-C	Pellet	0.8	25.0
Com-D	Extrudate	0.8	—
Com-E	Pellet	1.3	31.0

Note: g/cm^3 = grams per cubic centimeter; NiO = nickel oxide, wt% = weight percent.
[a] Standard FCC attrition test (Davison Index) target = 9.

4.1.2 RTI Catalyst Development Objectives

As shown in the high-pressure, bench fluidized-bed tests, many of the commercial catalysts possessed excellent methanation activity and selectivity. However, because these materials have been developed for fixed-bed applications, they exhibited high rates of attrition (Table 4-1) and are thus not suitable for long-term fluidized transport operation. The success of the novel CO_2 reuse process is dependent upon the development of a fluidizable Ni-based methanation catalyst that possesses both adequately high activity for meeting product gas specifications and sufficient strength for economically long life. Research and development activities in Phase I of the project were therefore focused on developing and optimizing two Ni-based catalyst formulations designed for fluidized applications.

4.1.3 Optimization of Cat-1 Synthesis Procedure

As stated in Section 3.1.1, two co-precipitation methods — the constant pH method and the raised pH method — were evaluated for the synthesis of Cat-1. The mixed-metal hydroxide precipitates formed from these techniques were then filtered, spray-dried, and calcined to produce a final particulate product for testing. Figure 4-2 presents the methanation performance of the Cat-1 catalysts made by the two synthesis routes. Both materials demonstrated reasonable methanation activity relative to the commercial materials with 100% CH_4 selectivity. Furthermore, because catalyst performance was not significantly impacted by the synthesis methodology, the raised-pH co-precipitation method was selected for further development because it provided an easier scale-up path. The parametric testing discussed below was used to systematically improve the catalytic performance and strength of Cat-1.

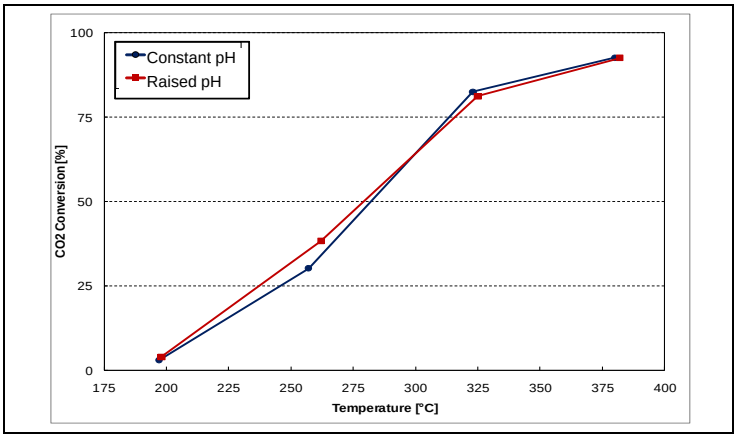

Figure 4-2. Methanation performance of Cat-1 synthesized by constant-pH and raised-pH co-precipitation methods. Both materials were spray-dried and calcined at 450 °C.

Precipitating Agent. To determine the effect of precipitating agents on catalyst properties, Cat-1 was prepared using two different precipitating agents, Na_2CO_3 and NH_4OH. As indicated by X-ray diffraction (XRD) and surface area analyses, the structural properties of the catalyst were not significantly affected by the choice of precipitating agent. (Total specific surface area was determined using the Brunauer, Emmett, and Teller [BET] equation.) The XRD patterns of Cat-1 prepared with NH_4OH and Na_2CO_3, were indistinguishable, as shown in Figure 4-3. The catalyst prepared with Na_2CO_3, though, had modestly higher BET surface area (260 m^2/g) than the material prepared with NH_4OH (227 m^2/g).

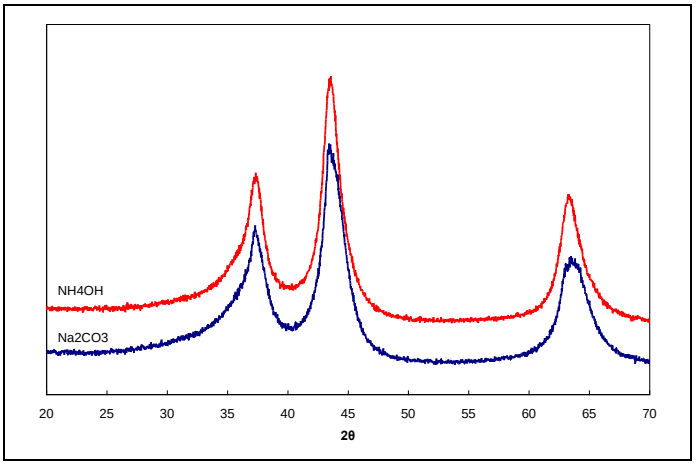

Figure 4-3. XRD patterns of Cat-1 synthesized with NH_4OH and Na_2CO_3.

The catalytic activity of Cat-1 materials, however, was significantly impacted by the choice of precipitating agent, given identical catalyst drying, calcining, and reducing conditions. The fluidized test results in Figure 4-4 show that the Cat-1 material prepared with Na_2CO_3 had much lower catalytic activity than the material prepared with NH_4OH. The lower activity of Cat-1 made with Na_2CO_3 is attributed to residual traces of sodium, which has a detrimental effect on the grain size and surface area of exposed metal following reduction of this Cat-1 formulation.

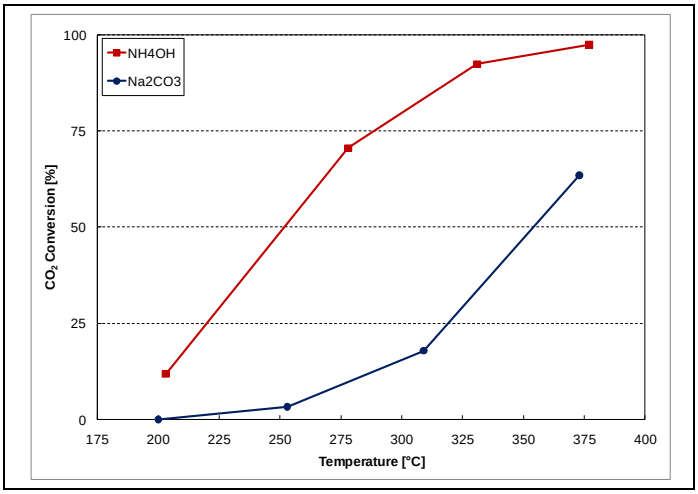

Figure 4-4. Effect of precipitating agent on CO_2 methanation activity of Cat-1.

In industrial catalyst manufacturing processes, Na_2CO_3 is the preferred precipitating agent because the gas-phase decomposition products during calcination are benign and do not require any further treatment. For subsequent Cat-1 syntheses in this Phase I project, NH_4OH was selected as the precipitating agent because this agent uses slightly different precipitation chemistry, limiting the sodium concentration in the final product.

Calcination Temperature. Green (spray-dried) particulates of Cat-1 were calcined at a temperature ranging from 350 to 450 °C. The Cat-1 catalytic activity, as measured by CO_2 conversion in Figure 4-5, increased significantly with decreasing calcination temperature. All Cat-1 samples showed nearly 100% CH_4 selectivity over the temperature range from 200 to 350 °C. Lower calcination temperatures also resulted in more methanation activity at 200 °C, as seen in Figure 4-5.

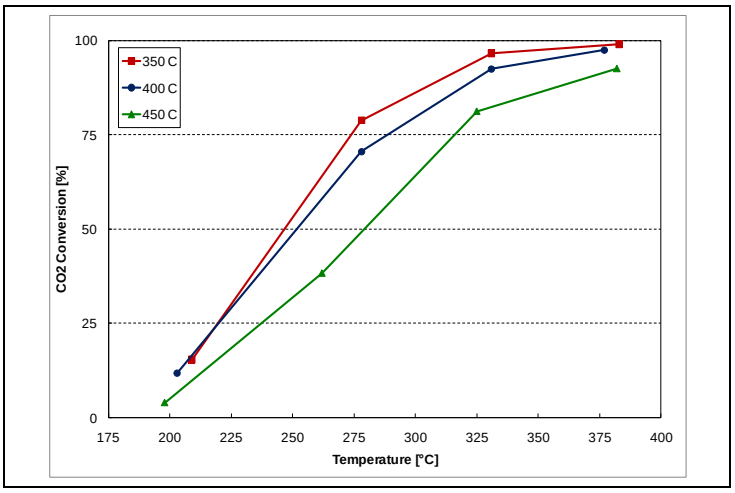

Figure 4-5. Effect of calcination temperature on Cat-1 methanation activity.

Aging Study. To evaluate Cat-1 performance stability, a 550-h aging study was completed using a fixed bed with a 1:10 mass mixture of catalyst to α-alumina. The temperature and space velocity (SV) ranges investigated were 250-350 °C and 9,000-15,000 h^{-1}, respectively. Results of the aging study are shown in Figure 4-6. At 250 °C and 9,000 h^{-1}, Cat-1 demonstrated almost 100% CO_2 conversion. To accelerate the aging process, the temperature was increased to 350 °C. At this higher temperature, Cat-1 showed stable activity for more than 150 h, indicating that the catalyst is resistant to thermal sintering. To further accelerate catalyst aging, the space velocity was increased to 15,000 h^{-1}. Though CO_2 conversion at this higher space velocity decreased as expected, stable catalyst performance was observed under these conditions for an additional 200 h, demonstrating that the Cat-1 formulation possesses excellent thermal stability. Analysis of gas and condensed products by GC and GC-MS, respectively, also showed essentially 100% selectivity toward methane with no traces of organic compounds in the condensed water.

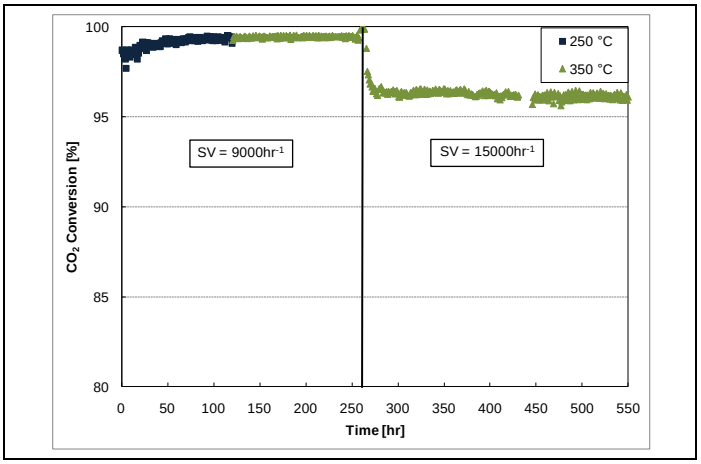

Figure 4-6. Methanation activity of Cat-1 over time.

4.1.4 Cat-1 Preparation Scale-Up

Cat-1 was selected to be produced in scaled-up amounts for testing in the pilot-plant reactor system after demonstrating excellent performance stability during extended bench-scale tests. A scaled Cat-1 synthesis procedure, based on the optimization results, was transmitted to Süd-Chemie, Inc. (SCI) for the manufacture of a 100-lb batch of this material in its pilot-plant facility in Louisville, KY. SCI

manufactured the pilot batch of Cat-1 material using the co-precipitation method with NH_4OH as the precipitating agent. The resulting slurry was spray-dried using a commercial spray dryer.

Before calcining the scaled Cat-1 batch, a sample of the green particulate product (post-spray drying but prior to calcination) was sent to RTI for evaluation. After calcination at 350 and 400 °C, the activity of the green scaled material was evaluated in RTI's bench-scale reactor. As shown in Figure 4-7, the scaled Cat-1 material calcined at 350 °C had very similar performance to its laboratory counterpart over the reaction temperature range investigated. However, the scaled material calcined at 400 °C showed much lower performance than the laboratory version at reaction temperatures below 350 °C. This unexplained result shows how preparation procedures, precipitation chemistry, spray-drying and calcination conditions, and reduction interact to greatly influence the Cat-1 catalytic activity. More importantly, though, these results show that the scaled synthesis procedure did successfully produce a Cat-1 material having performance similar to that of the laboratory-prepared material. Based on these results, the calcination temperature for the 100-lb batch of scaled Cat-1 was selected to be 350 °C.

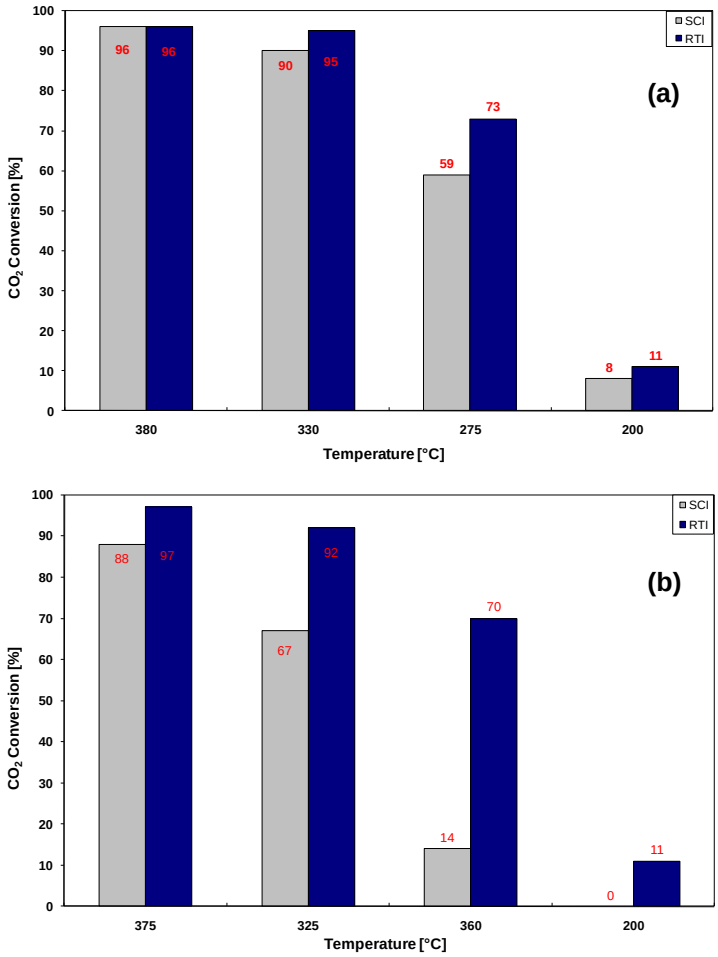

Figure 4-7. Performance comparison of commercial and laboratory-prepared Cat-1 catalysts calcined at (a) 350 °C and (b) 400 °C.

4.1.5 Cat-3 Development

As part of the Phase I catalyst development effort, a second fluidizable, Ni-based catalyst formulation, Cat-3, was also prepared. The Cat-3 formulation is a precipitated mixture of NiO, ZrO_2, and CeO_2 with Ni:Zr:Ce molar ratio of 6:3:1. It was selected because of the oxidation and reduction interactions of ZrO_2 with catalytic materials, such as Ni, at low temperature to yield more active catalytic sites and CeO_2 to enhance reactions with CO_2. The constant-pH preparation method was used to synthesize Cat-3 because it was expected to yield a more uniform catalyst.

The parametric testing of Cat-3 evaluated the effects of calcination temperature and precipitating agent on catalyst performance. The calcination temperature range explored was 400-550 °C, and NH_4OH, NaOH, and Na_2CO_3 were evaluated as precipitation agents. As observed previously for Cat-1, Figure 4-8 shows that the precipitating agent used significantly affected the Cat-3 catalytic performance. Using Na_2CO_3 dramatically increased catalyst activity, while maintaining 100% CH_4 selectivity. Although the Cat-3 material precipitated with Na_2CO_3 was calcined at a lower temperature, it is noted that the precipitating agent had a greater effect on material performance than the calcination temperature, as determined from a calcination temperature study on the Cat-3 material made with Na_2CO_3. The effect of calcination temperature on the Cat 3 methanation performance is plotted in Figure 4-9. Like Cat-1, Cat-3 exhibited improved methanation activity with decreasing calcination temperature. One significant difference is that Cat-3 was more active than Cat-1 at higher calcination temperatures.

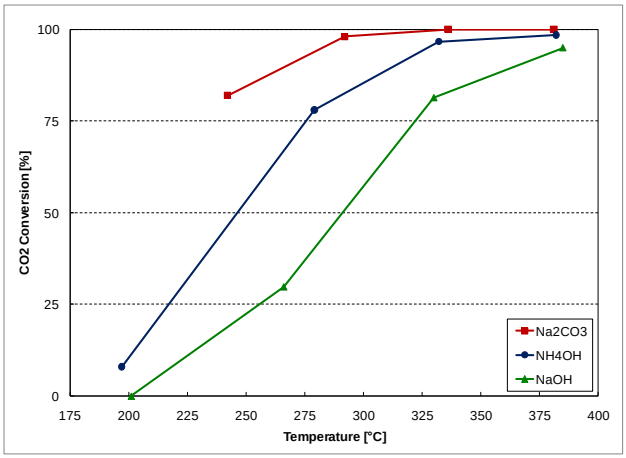

Figure 4-8. Effect of precipitating agent on methanation activity of Cat-3.

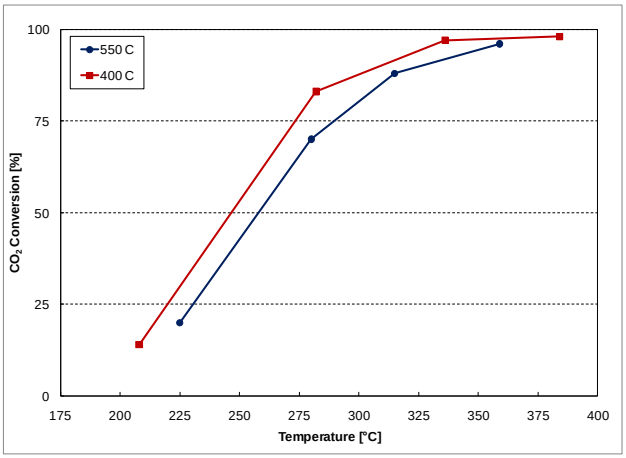

Figure 4-9. Effect of calcination temperature on methanation activity of Cat-3 made with Na_2CO_3.

4.1.6 Cat-3 Preparation Scale-Up

To evaluate scalability of the Cat-3 synthesis procedure, a scaled Cat-3 synthesis procedure, based on the optimization results, was provided to SCI for the manufacture of a 100-lb batch of this material in their pilot-plant facility. SCI manufactured the Cat-3 catalyst using Na_2CO_3 as the precipitating agent and calcined it at 400 °C. The slurry was spray-dried using a commercial spray dryer.

The catalytic performance of the commercially prepared Cat-3 catalyst is compared to that of the corresponding laboratory-prepared material in Figure 4-10. At reaction temperatures below 350 °C, the scaled Cat-3 material had much lower performance than the laboratory material. These results are similar to the scaled Cat-1 results (Section 4.1.4), which also showed that 400 °C calcination yielded a lower-performing catalyst.

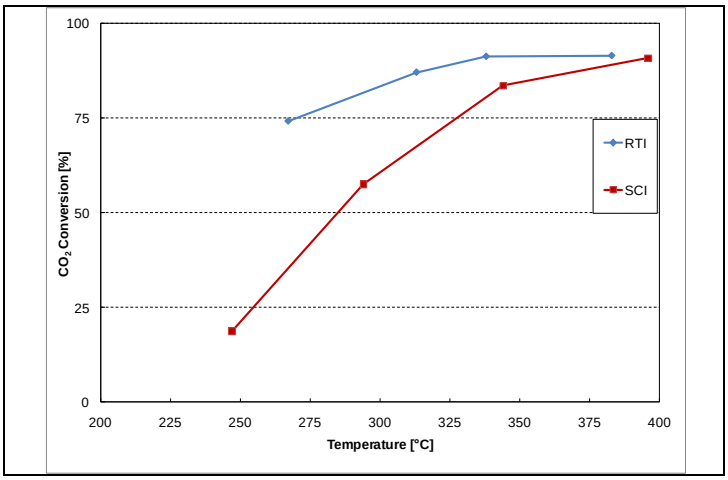

Figure 4-10. Performance of commercial and laboratory-prepared Cat-3 catalysts at H_2/CO_2 ratio of 6:1.

Testing with Stoichiometric Concentrations of CO_2 and H_2. To understand their equilibrium methanation activity, RTI's fluidizable, Ni-based Cat-1 and Cat-3 catalysts were evaluated using the stoichiometric feed H_2/CO_2 ratio of 4:1. Except for this H_2/CO_2 ratio, all other reaction conditions were the same as in previous tests. The results are compared to the equilibrium methanation performance of several best-performing commercial methanation catayst in Figure 4-11. The performance activity of both fluidizable Cat-1 and Cat-3 materials are seen to be comparable or exceed that of the commercial (fixed-bed) methanation catalysts. Even at stoichiometric conditions, RTI's Cat-3 showed better methanation activity than the commercial materials, achieving more than 80% CO_2 conversion at temperatures below 300 °C. Based on these data, the Phase I catalyst development work has resulted in the development of two promising fluidizable, Ni-based catalyst formulations, Cat-1 and Cat-3.

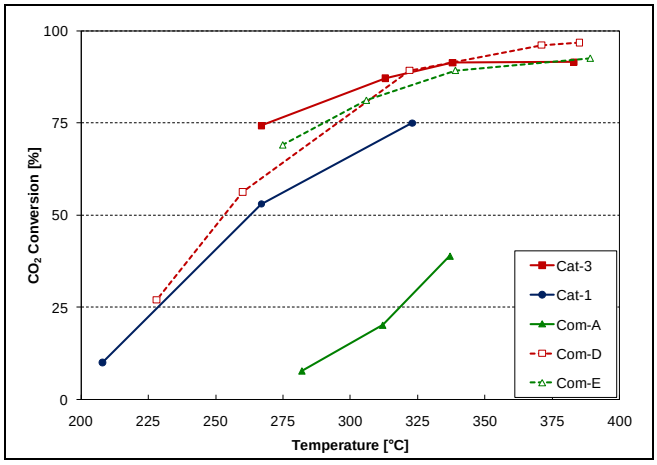

Figure 4-11. Performance comparison of RTI's Cat-1 and Cat-3 catalysts with commercial methanation catalysts at H_2/CO_2 ratio of 4:1.

4.2 Computational Fluid Dynamics Modeling

As a part of this Phase I project, preliminary CFD modeling was completed to understand the hydrodynamics of the transport reactor system for the CO_2 reuse reaction. The main objectives of the CFD modeling effort were to estimate

- CO_2 conversion profile across the reactor length
- Single-pass CO_2 conversion that can be achieved in a riser reactor
- Ability to use solids-to-gas ratio to limit temperature rise across the riser to <400 °C

A preliminary two-dimensional CFD model of the riser was developed using Ansys Fluent®. The model consisted of a vertical reactor of uniform cross-section with gas and solids entering at the reactor bottom and the reaction products leaving from the top of the reactor. Table 4-2 gives the relevant reactor dimensions, physical properties, and modeling conditions used in the CFD simulation. The gas flow and composition were based on a 4-ton/day pilot unit design for Phase II of the project. Based on our preliminary design calculations, the riser had a diameter of 2 in. and total height of 60 ft.

In the CFD simulations, the Sabatier reaction ($CO_2 + 4H_2 = CH_4 + 2H_2O$) was assumed to be the only reaction occurring inside the riser. The surface reaction rate for this reaction was calculated using Equations 2-4:

$$r = k_1 P_{CO_2} P_{H_2}^{0.5} / \left(P_{H_2}^{0.5} + k_2 P_{CO_2}\right) \quad [2]$$

$$k_1 = 1.46 \times 10^9 e^{(-9{,}460/T)} \text{ mmol/(g·h·kPa)} \quad [3]$$

$$k_2 = 1.18 \times 10^{-3} e^{(3{,}710/T)} \text{ kPa}^{-0.5} \quad [4]$$

where P_{CO_2} and P_{H_2} are the partial pressures [kPa] of CO_2 and H_2, respectively, and T is the reactor temperature [K].

The catalyst distribution and CO_2 concentration and conversion profiles obtained from the CFD simulation are shown along the reactor height in Figure 4-12 and Figure 4-13. About 98% of the CO_2 was converted to methane in the first 3 meters (~10 ft.) of the reactor. The riser gas temperature profile shown in Figure 4-14 indicates that the temperature increased by about 150 °C in the first 5 meters (~16 ft.) of the riser. The most rapid temperature increase occurred between 2 and 3 meters (7 and 10 ft.), which also corresponded to the region with the greatest CO_2 conversion. The gas temperature continued to increase for an additional 2 meters (7 ft.) because of heat transfer from the solid (where the reaction was occurring) to the gas surrounding the particles. For comparison, the temperature rise in an adiabatic, fixed-bed reactor would be 540 °C under these same modeling conditions. Thus, these CFD results confirmed our hypothesis that the large thermal mass of solids circulating through the riser can effectively control the temperature rise in the riser while achieving high single-pass conversion.

The CFD modeling results also show that reactivity of the current catalyst was rapid enough to achieve almost complete conversion in a very short residence time or in a small fraction of the total reactor height. This presents opportunities for increasing gas throughput without reducing conversion, reducing reactor size, and/or using potentially less active catalysts. In particular, the option of using less active catalysts suggests that some catalyst chemical activity could be sacrificed for improved catalyst attrition resistance.

Table 4-2. CFD Simulation Conditions and System Properties

Reactor Dimensions	
Height	18.3 m (60 ft.)
Diameter	5.1 cm (2 in.)
Material Properties	
Gas (mixture of CO_2, H_2, CH_4, and H_2O)	Incompressible ideal gas
Thermal conductivity	Mass-weighted average
Specific heat	Mass-weighted average
Viscosity	Mass-weighted average
Catalyst	
Particle diameter	80 μm
Specific heat	940 J/(mol·K)
Thermal conductivity	130 W/(m·K)
Molecular weight	42.84
Operating Conditions	
Pressure	21.7 bar (314.7 psi)
Temperature	250 °C
Superficial gas velocity	3.0 m/s (10 ft/s)
Solids/gas mass ratio	20:1
Feed gas composition (mole fraction)	
CO_2	0.1851
H_2	0.7317
CH_4	0.0832
Initial Conditions in Domain	
Gas velocity	0
Catalyst velocity	0
Catalyst volume fraction	0
Composition of gas (mole fraction)	
CO_2	0.1851
H_2	0.7317
CH_4	0.0832
Boundary Conditions	
Gas	No slip
Catalyst	Johnson Jackson BC
Mesh Size	
No. of cells	60,000
Convergence Criterion	10^{-4}
Step Size	0.001 s

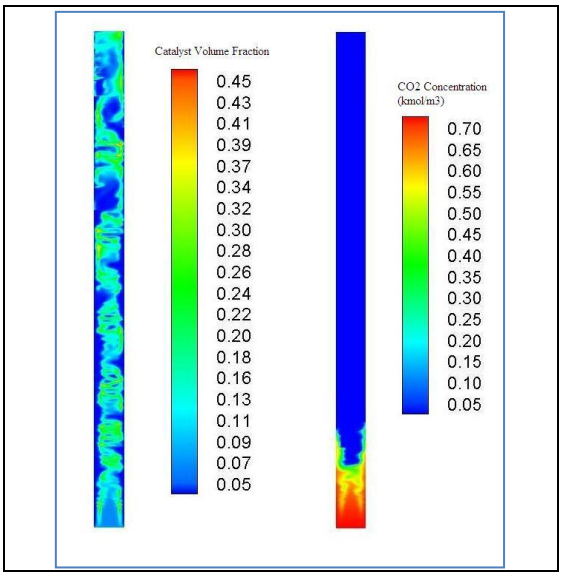

Figure 4-12. CO_2 concentration distribution in the transport reactor modeled.

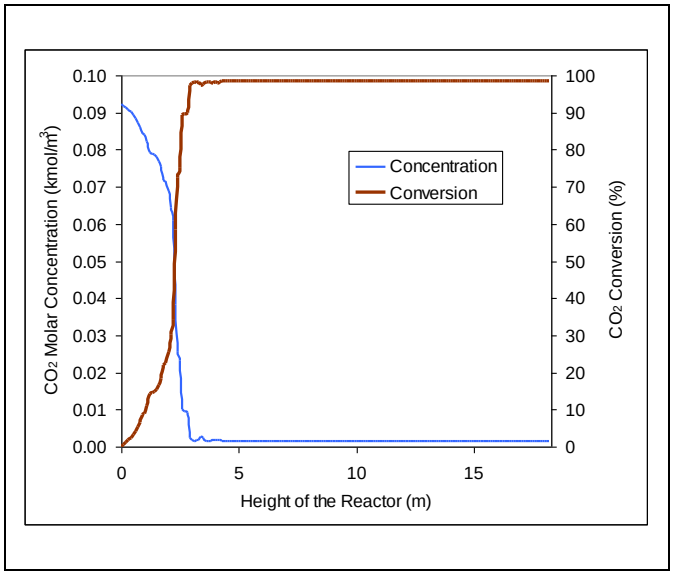

Figure 4-13. Average CO_2 concentration and conversion along the transport-reactor height.

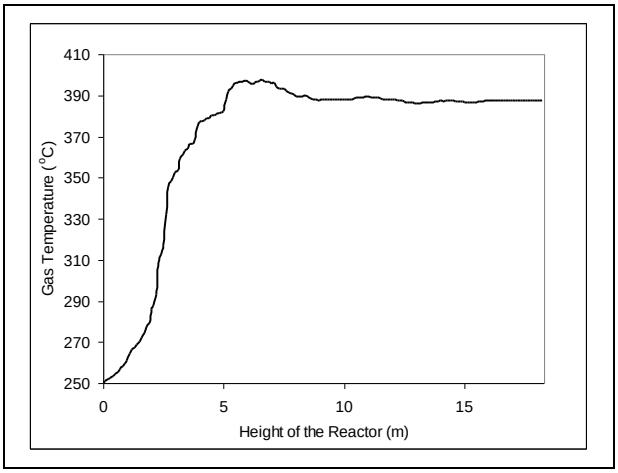

Figure 4-14. Average gas temperature along the transport reactor height.

4.3 Pilot-Scale Transport Reactor Testing of Methanation Catalysts

To test the efficacy of using a fluidizable Ni-based methanation catalyst in a transport reactor, the methanation performance of Cat-1 was evaluated in a transport reactor system. Specifically, the scaled 100-lb. batch of Cat-1 manufactured by SCI in their pilot-plant production facility was evaluated in the FCC reactor test unit at KBR's Technology Center in Houston, TX. The testing objectives were to demonstrate the catalytic activity of Cat-1 and the ability to achieve high single-pass conversion and temperature control using the circulating solids in the reactor.

KBR's FCC reactor system, shown in Figure 4-15, consists of a single circulation loop composed of a riser (80 ft. of 0.25-in.-dia. SCH 40 pipe), a high-efficiency cyclone, a stripper, and a regenerator. A 1.5-gallon (5.67-L) charge of Cat-1 was loaded into the FCC regenerator and evaluated in this pilot system at 200-300 °C, a system pressure of 35 psig, and a superficial gas velocity range of 10-20 ft/s (3-9 m/s). During operation, the outlet H_2, CO_2, CH_4, and N_2 concentrations were measured every 15 minutes with a Varian 3300 gas chromatograph. The simulated fuel-gas composition used in parametric testing consisted of 20 vol% CO_2 and 80 vol% H_2 and was chosen to evaluate the most stringent methanation and thermal load cases possible.

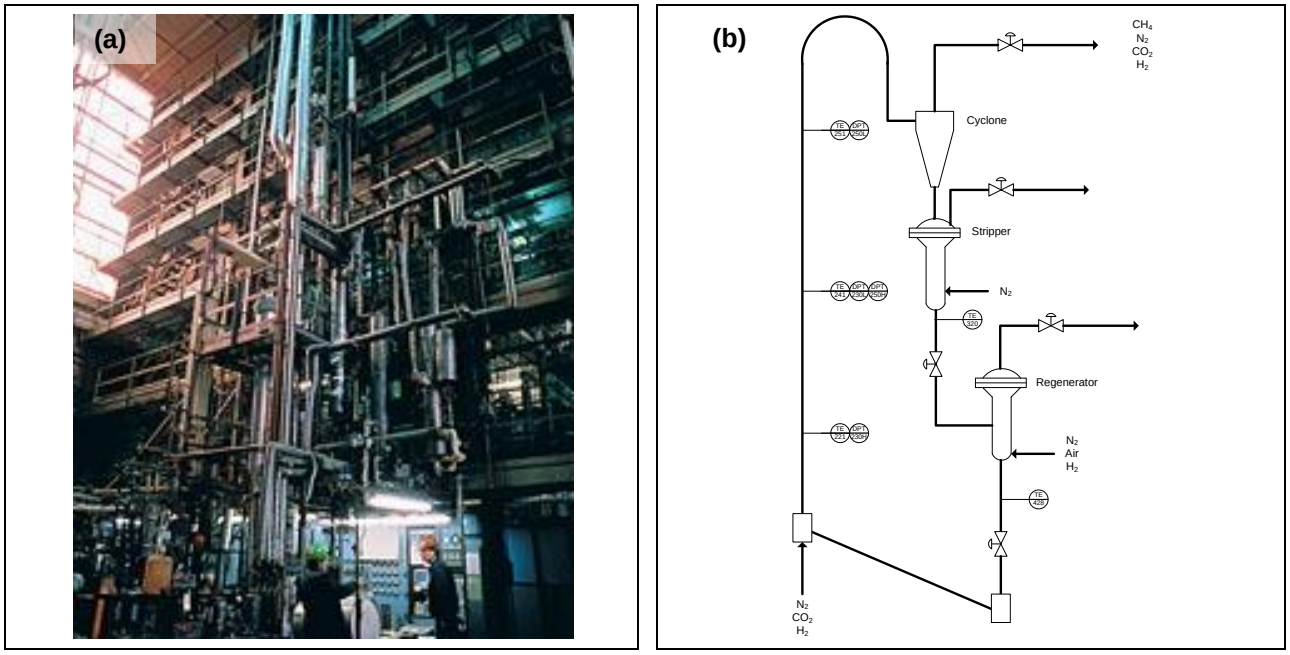

Figure 4-15. (a) Photo and (b) schematic of the FCC pilot plant system at KBR's Technology Center.

Figure 4-16 plots the measured differential pressures across the riser [see Figure 4-15(b) for locations of differential taps] at a superficial gas velocity of 10 ft/s (3 m/s) during initial attempts to circulate the catalyst. The observed differential-pressure fluctuations are typical of a transport reactor system. The relatively narrow deviation of the differential pressure around the average reflects stable catalyst circulation with no evidence of slugging.

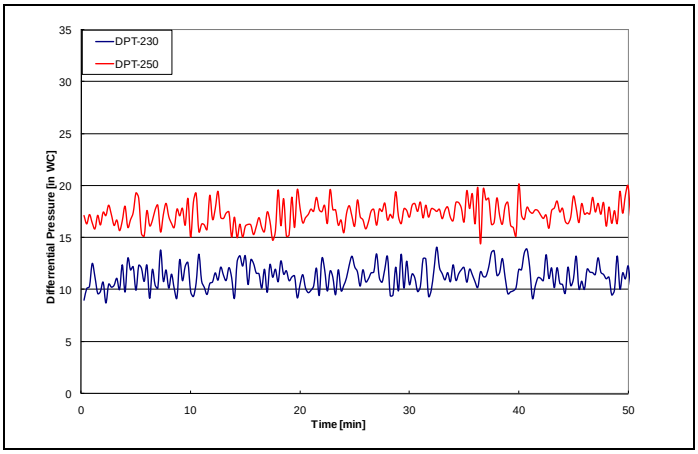

Figure 4-16. Riser differential pressures during circulation.

Table 4-3 summarizes the Cat-1 testing results in KBR's pilot FCC test unit. In all eleven trials completed at the indicated test conditions, Cat-1 achieved high CO_2 conversion in a single pass. Its selectivity for methane was also very high, with the lowest methane selectivity being 99.4%. Because the equilibrium CO_2 conversion for the Sabatier reaction ($CO_2 + 4\ H_2 = CH_4 + 2\ H_2O$) at 200 and 300 °C is 99.3 and 96.9%, respectively, the performance test data show that Cat-1 was able to achieve near-equilibrium CO_2 conversion for gas residence times between 4 and 8 seconds.

Table 4-3. Pilot Plant Test Results

Trial No.	Riser Inlet Temperature (°C)	Riser Gas Velocity (ft/s)	Average CO_2 Conversion (%)	CH_4 Selectivity (%)
1	300	10	95.0	99.8
2	300	15	95.1	99.5
3	300	20	94.6	99.7
4	300	10	94.9	99.7
5	275	10	94.3	99.8
6	275	20	93.9	99.5
7	200	10	93.4	99.7
8	200	15	93.2	99.8
9	200	20	92.5	99.4
10	250	10	94.2	99.7
11	250	20	93.7	99.6

Figure 4-17 shows the temperature rise seen across the riser during Trial 3. [The positions of the three thermocouples in the riser are indicated in Figure 4-15(b).]. A rapid temperature rise of approximately 17 °C occurred when the fuel-gas mixture was introduced into the riser. The CO_2 conversion during Trial 3 was 95%. For comparison, the temperature rise for the same CO_2 conversion in a fixed-bed reactor would be approximately 450 °C. This result experimentally validates the CFD modeling data (Section 4.2) that indicated that the thermal mass of the circulating solids should provide an effective means of controlling temperature rise.

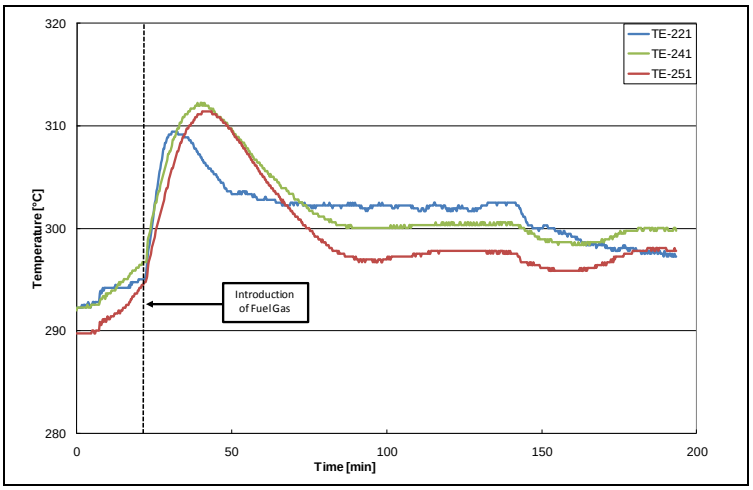

Figure 4-17. Riser temperature measured during methanation Trial 3.

The testing in KBR's FCC reactor system also demonstrated the ability to remove sensible heat from the circulating solids. Figure 4-18 presents the solids temperature exiting the riser, stripper, and regenerator [see Figure 4-15(b) schematic for the thermocouple locations]. During this testing, a high N_2 flow was used in the stripper and regenerator to cool the solids by removing sensible heat. As shown in Figure 4-18, the catalyst leaving the stripper and regenerator was significantly cooler than the catalyst entering the stripper, indicating that a solids cooler should be very effective for extracting the sensible heat from the circulating solids (i.e., "regenerating" the thermal mass of the circulating solids).

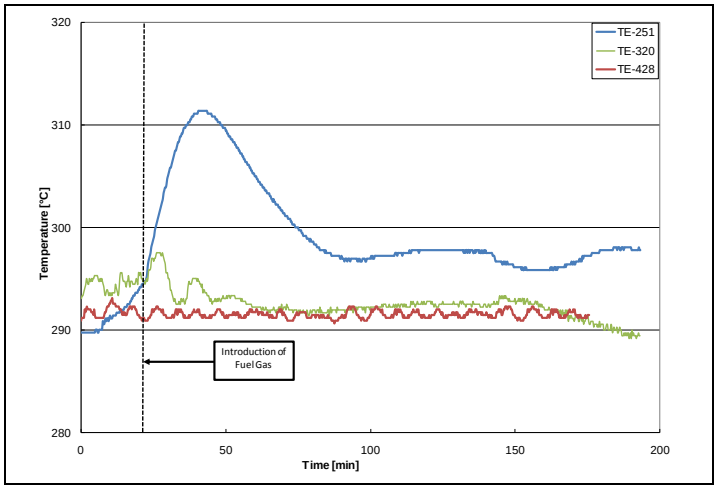

Figure 4-18. Comparison of catalyst temperatures exiting the riser, stripper, and regenerator.

Extended performance testing of Cat-1 in KBR's FCC test unit was conducted with two different fuel-gas compositions — Gas A composed of 80 vol% H_2 in balance CO_2 and Gas B composed of 73.5 vol% H_2, 18.2 vol% CO_2, and balance CH_4. The Gas B composition was chosen to evaluate the inhibiting effect of CH_4 in the inlet feed. Figure 4-19 presents the CO_2 conversion at 200, 250, and 300 °C at a riser gas velocity of 10 ft/s for both test gases. During the first 7 hours of testing in Gas A at 300 °C, the CO_2 conversion gradually increased from 82 to 97% [Figure 4-19(a)]. This increase in activity indicated that the catalyst activation process in which NiO is reduced to elemental Ni had been incomplete so that the catalyst continued to be reduced during initial testing. This hypothesis was confirmed in the subsequent tests with Gas B, in which the same catalyst sample was used and did not exhibit this gradual activity increase [Figure 4-19(b)]. After complete activation, Cat-1 consistently demonstrated 93% or greater CO_2 conversion. Equilibrium CO_2 conversion with Gas B at 200 and 300 °C is 99.8 and 97.1%, respectively. The extended test results with Gas B clearly show that the presence of CH_4 in the feed did not inhibit the methanation activity of Cat-1 and its ability to produce near pipeline-quality SNG in a single pass.

The material properties of fresh and spent samples of the scaled Cat-1 catalyst used in the pilot testing were characterized. As shown in Table 4-4, the scaled Cat-1 material maintained its surface area throughout extended testing, consistent with the stable activity seen in Figure 4-19. The reduction in Cat-1 particle size was a result of mechanical attrition caused by the catalyst circulation in the pilot transport reactor. From these results, the scaled Cat-1 material generated fines at a rate 2-4 times greater than a commercial FCC material.

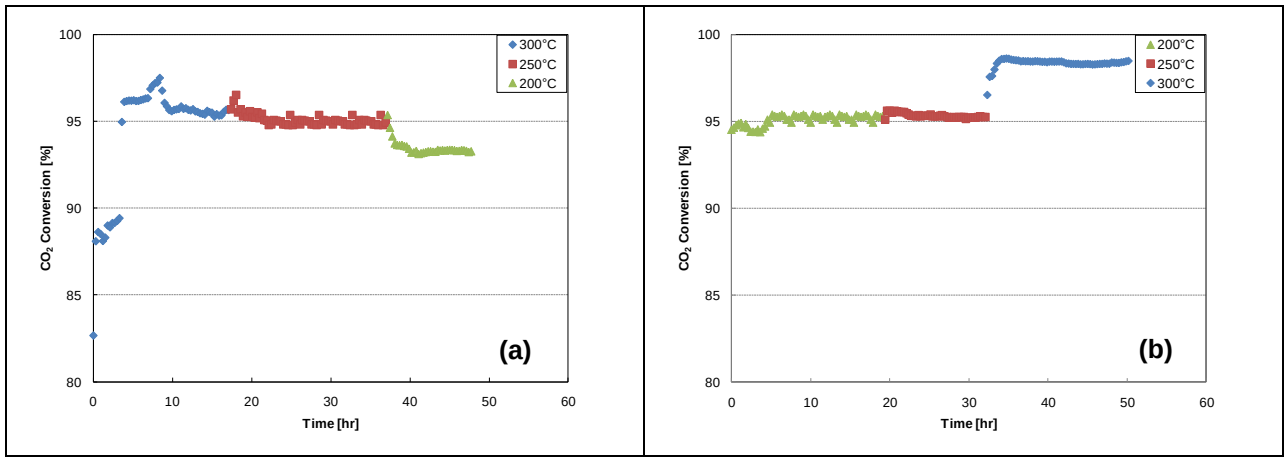

Figure 4-19. Cat-1 methanation performance in extended testing in KBR's pilot FCC system with (a) Gas A and (b) Gas B.

Table 4-4. Fresh and Spent Catalyst Properties of Scaled Cat-1

Catalyst Property	Fresh Cat-1	Spent Cat-1
BET surface area (m^2/g)	174	147
Bulk density (g/ml)	1.2	1.2
Davison attrition ratio[1]	2.2	3.6
Particle size distribution		
<10 µm	0	3.4
<20 µm	0	15.5
<30 µm	0	47.1

[1] Relative ratio of measured attrition loss for material compared to that of fresh FCC catalyst.

In summary, the pilot transport-reactor test results successfully demonstrated the key advantages of RTI's TRM process over conventional commercial methanation technologies. The parametric and extended tests showed that the TRM process can achieve high single-pass conversion and convert ethylene-plant fuel-gas mixtures into pipeline-quality SNG. The novel concept of using a fluidizable catalyst to absorb the heat generated by an exothermic reaction was validated by the limited temperature rise seen across the transport reactor. Additionally, the ability to use a solids cooler to remove the latent heat generated by the methanation reaction as sensible heat from the circulating catalyst was shown. The combination of these results demonstrate the potential of the TRM process to significantly intensify process configuration and minimize process footprint by utilizing a single transport reactor to convert ethylene fuel-gas streams into pipeline-quality SNG.

5. Preliminary Engineering Package

As one of the key objectives for Phase I, RTI developed a basic engineering design (BED) package for the pilot demonstration unit of RTI's CO_2 reuse process to be integrated into a host site in the next project phase. The primary goal of the BED package was to determine the cost of a pilot demonstration unit of RTI's CO_2 reuse process for converting approximately 4 tons per day of CO_2 into pipeline-quality SNG at a field host site. The BED package consisted of a process description, a PFD, heat and material balances, and a ±30% preliminary economic analysis.

5.1 Process Description

The PFD for the pilot demonstration unit for RTI's CO_2 reuse process is shown in Figure 5-1. The corresponding material and energy balances are given in Tables 5-1 through 5-5. This unit was designed to convert 4 tons/day of CO_2 into pipeline-quality SNG at a production rate of 4,363 lb/day of SNG. As shown in Figure 5-1, fuel gas from an ethylene production plant (Stream 1) was mixed with CO_2 (Stream 3) to form the inlet gas to the CO_2 reuse process unit. The CO_2 for Stream 3 was separated from a flue-gas stream (Stream 2) in the CO_2 recovery unit. The flow rate, composition (in mole fraction), temperature, and pressure of Streams 1 and 3 are provided in Table 5-6.

The combined stream of Streams 1 and 3 to the pilot demonstration unit for the CO_2 reuse process was then compressed by centrifugal compressor (C-100) to the reaction pressure and to overcome downstream pressure drop. Downstream of the transport reactor (R-200), the primary process equipment contributing to the pressure drop included heat exchangers HX-200, HX-201, and HX-300 and the molecular-sieve dryers (V-304/305). Thus, the fuel-gas compressor C-100 was designed for an outlet pressure of 319.7 psia to meet these reactor pressure and pressure drop specifications. This compressor comprised four stages with intercoolers using cooling water to lower the next-stage inlet stream temperature to 38 °C (100 °F). The resulting fuel gas (Stream 5) exited the C-100 compressor at approximately 319.7 psia and then entered the feed gas heater HX-200, where it was heated to the R-200 reactor inlet temperature of 250° C (482 °F). During start-up, nitrogen (Stream 23) was used to preheat the reactor system to the desired temperature by flowing it through the electric start-up heater (HX-202) before entering (R-200).

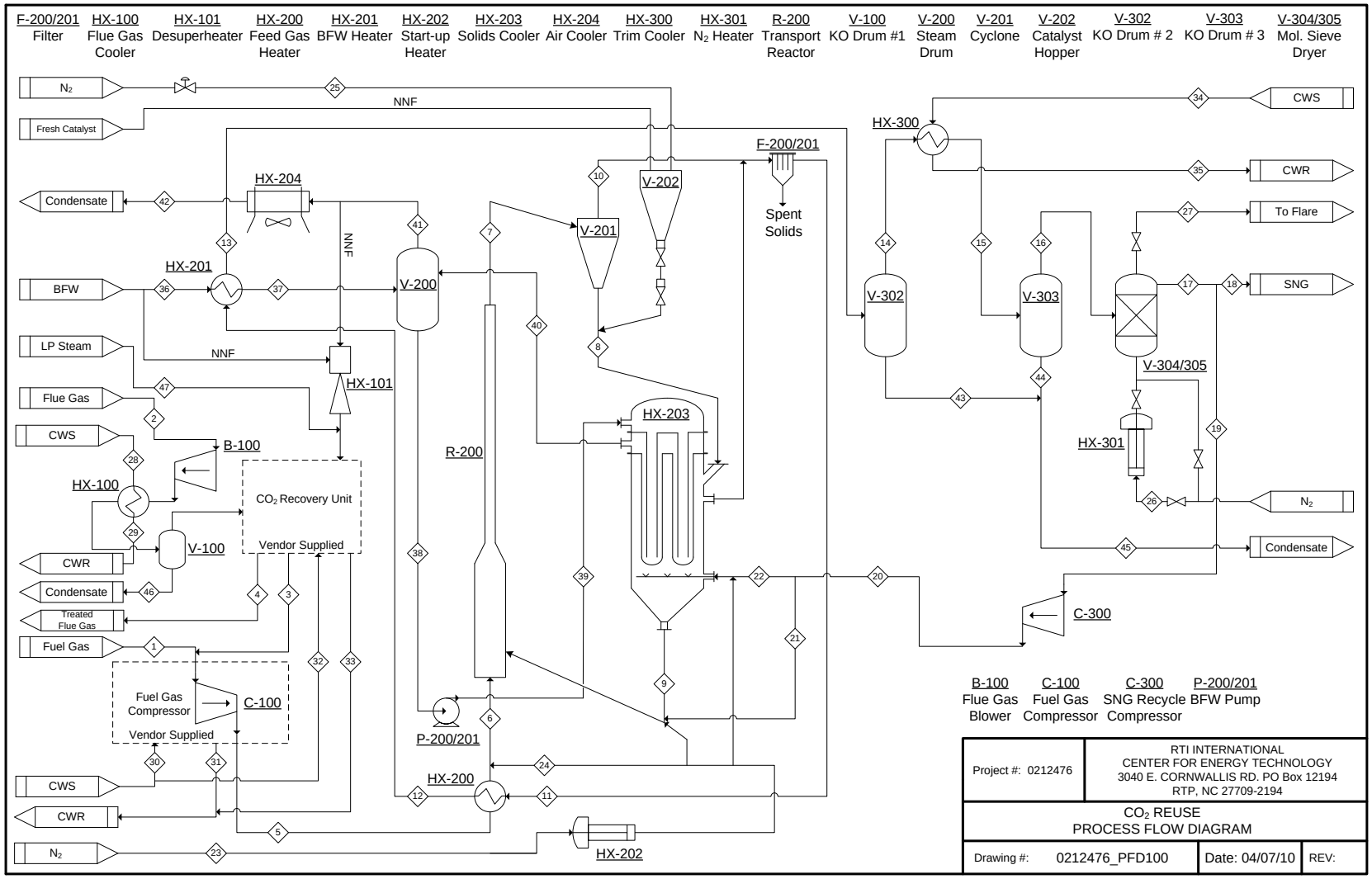

Figure 5-1. Process flow diagram (PFD) of RTI's CO_2 reuse process.

Table 5-1. CO_2 Reuse Pilot-Plant Process Material and Energy Balances (Streams 1-11)

Stream ID			1	2	3	4	5	6	7	8	9	10	11
Stream Description		Units	FUEL GAS TO C-100	FLUE GAS TO CO_2 RECOVERY	CO_2 TO C-100	TREATED FLUE GAS FROM CO_2 RECOVERY	FUEL GAS TO HX-200	FUEL GAS TO R-200	OFF-GAS TO V-201	SOLIDS TO HX-203	SOLIDS TO R-200	OFF-GAS TO F-200/201	OFF-GAS TO HX-200
Temperature		°F	100.0	135.0	100.0	105.9	296.1	482.0	572.0	572.0	482.0	571.6	571.6
Pressure		psia	14.7	14.7	14.7	16.5	319.7	314.7	309.7	309.7	314.7	309.7	309.7
Molar Flow Rate		lb-mol/h	33.4	57.8	7.6	42.6	40.9	40.9	652.0	621.5	625.9	38.0	37.9
Mass Flow Rate		lb/h	115	1,659	333	1,172	448	448	27,145	26,626	26,696	640	637
Molecular Weight			3.448	28.718	44.010	27.521	10.955	10.955	41.630	42.840	42.652	16.852	16.809
HHV		Btu/scf	395.23	0.00	0.00	0.00	322.09	322.09	23.54	0.00	6.85	593.73	594.71
Fraction Vapor			1.00	1.00	1.00	1.00	1.00	1.00	0.80	0.00	0.00	1.00	1.00
TOTAL STREAM Composition	MW												
H_2O	18.015	lb-mol/h	0.000	9.071	0.000	2.555	0.000	0.000	14.797	0.000	0.000	14.797	14.797
N_2	28.013	lb-mol/h	0.000	39.604	0.000	38.889	0.000	0.000	0.000	0.000	0.000	0.000	0.000
O_2	31.999	lb-mol/h	0.000	1.185	0.000	1.129	0.000	0.000	0.000	0.000	0.000	0.000	0.000
CO_2	44.010	lb-mol/h	0.000	7.916	7.575	0.000	7.575	7.575	0.245	0.000	0.068	0.360	0.360
SO_2	64.070	lb-mol/h	0.000	0.002	0.000	0.000	0.000	0.000	0.000	0.000	0.000	0.000	0.000
H_2	2.016	lb-mol/h	29.950	0.000	0.000	0.000	29.950	29.950	0.495	0.000	0.138	0.727	0.727
CH_4	16.043	lb-mol/h	3.405	0.000	0.000	0.000	3.405	3.405	14.993	0.000	4.190	22.018	22.018
Catalyst	42.840	lb-mol/h	0.000	0.000	0.000	0.000	0.000	0.000	621.519	621.519	621.519	0.062	0.000
VAPOR PHASE													
Mass Flow Rate		lb/h	115	1,659	333	1,172	448	448	519		71	637	637
Act. Rate		ACFM	227.23	417.42	51.33	260.81	17.42	22.05	17.82		2.35	22.23	22.23
Std. Rate (60 °F, 14.696 psia)		MMSCFD	0.304	0.525	0.069	0.387	0.375	0.375	0.272		0.040	0.340	0.340
Molecular Weight			3.448	28.718	44.010	27.521	10.955	10.955	16.996		16.037	16.809	16.809
Density		lb/ft^3	0.008	0.066	0.108	0.075	0.429	0.339	0.485		0.500	0.478	0.478
C_p/C_v			1.391	1.366	1.287	1.396	1.349	1.330	1.265		1.225	1.251	1.251
Compressibility (Z)			1.000	0.999	0.995	0.999	1.006	1.007	0.980		0.999	0.985	0.985
Heat capacity, C_p		Btu/lb°F	2.051	0.260	0.207	0.256	0.720	0.741	0.626		0.713	0.649	0.649
Thermal Conductivity		Btu/hrft°F	0.091	0.015	0.010	0.015	0.085	0.103	0.037		0.042	0.039	0.039
Viscosity		cP	0.010	0.018	0.016	0.018	0.017	0.021	0.022		0.018	0.021	0.021
LIQUID PHASE													
Mass Flow Rate		lb/h											
Act. Rate		gpm											
Molecular Weight													
Density		lb/ft^3											
Heat capacity, C_p		Btu/lb°F											
Thermal Conductivity		Btu/hrft°F											
Viscosity		cP											
Surface Tension		dyne/cm											
SOLID PHASE													
Mass Flow Rate		lb/h							26,626	26,626	26,626	3	
Molecular Weight									42.840	42.840	42.840	42.840	
Density		lb/ft^3							99.885	99.885	99.885	99.885	
Heat capacity, C_p		Btu/lb°F							0.225	0.225	0.225	0.225	

Notes:

1. Flow of nitrogen during reactor start-up. Nitrogen flow is intermittent.
2. Flow of nitrogen during repressurization of V-202. Repressurization flow shown is larger flow. Nitrogen flow is intermittent.
   - Repressurization after addition of solids occurs once every 21 days with a flow of 23.56 SCFM.
   - Repressurization due to solids addition to reactor system occurs once every 2 days with a flow of 19.10 SCFM.
3. Flow of nitrogen during desorption process. Nitrogen flow is intermittent.

Table 5-2. CO_2 Reuse Pilot-Plant Process Material and Energy Balances (Streams 12-22)

Stream ID			12	13	14	15	16	17	18	19	20	21	22
Stream Description		Units	OFF-GAS TO HX-201	OFF-GAS TO V-302	OFF-GAS TO HX-300	OFF-GAS TO V-303	OFF-GAS TO V-304/305	SNG FROM V-304/305	SNG TO OSBL	SNG TO C-300	SNG FROM C-300	SNG TO R-200	SNG TO HX-203
Temperature		°F	418.9	320.0	320.0	100.0	100.0	100.0	100.0	100.0	116.7	116.7	116.7
Pressure		psia	299.7	294.7	294.7	289.7	289.7	289.7	289.7	289.7	319.7	319.7	319.7
Molar Flow Rate		lb-mol/h	37.9	37.9	34.0	34.0	23.2	23.1	11.3	11.8	11.8	4.4	7.4
Mass Flow Rate		lb/h	637	637	566	566	372	371	182	189	189	71	118
Molecular Weight			16.809	16.809	16.670	16.670	16.044	16.037	16.037	16.037	16.037	16.037	16.037
HHV		Btu/scf	594.71	594.71	663.34	663.34	972.24	975.52	975.60	975.62	975.62	975.51	975.55
Fraction Vapor			1.00	0.90	1.00	0.68	1.00	1.00	1.00	1.00	1.00	1.00	1.00
TOTAL STREAM	MW												
Composition													
H_2O	18.015	lb-mol/h	14.797	14.797	10.875	10.875	0.078	0.000	0.000	0.000	0.000	0.000	0.000
N_2	28.013	lb-mol/h	0.000	0.000	0.000	0.000	0.000	0.000	0.000	0.000	0.000	0.000	0.000
O_2	31.999	lb-mol/h	0.000	0.000	0.000	0.000	0.000	0.000	0.000	0.000	0.000	0.000	0.000
CO_2	44.010	lb-mol/h	0.360	0.360	0.360	0.360	0.360	0.360	0.176	0.183	0.183	0.068	0.115
SO_2	64.070	lb-mol/h	0.000	0.000	0.000	0.000	0.000	0.000	0.000	0.000	0.000	0.000	0.000
H_2	2.016	lb-mol/h	0.727	0.727	0.727	0.727	0.727	0.727	0.357	0.370	0.370	0.138	0.232
CH_4	16.043	lb-mol/h	22.018	22.018	22.017	22.017	22.016	22.016	10.802	11.215	11.215	4.190	7.025
Catalyst	42.840	lb-mol/h	0.000	0.000	0.000	0.000	0.000	0.000	0.000	0.000	0.000	0.000	0.000
VAPOR PHASE													
Mass Flow Rate		lb/h	637	566	566	372	372	371	182	189	189	71	118
Act. Rate		ACFM	19.32	15.53	15.53	7.73	7.73	7.71	3.78	3.93	3.67	1.37	2.30
Std. Rate (60 °F, 14.696 psia)		MMSCFD	0.336	0.299	0.299	0.204	0.204	0.203	0.100	0.103	0.104	0.039	0.065
Molecular Weight			16.809	16.670	16.670	16.044	16.044	16.037	16.037	16.037	16.037	16.037	16.037
Density		lb/ft^3	0.550	0.608	0.608	0.802	0.802	0.801	0.801	0.801	0.858	0.858	0.858
C_p/C_v			1.288	1.309	1.309	1.356	1.356	1.355	1.355	1.355	1.352	1.352	1.352
Compressibility (Z)			0.972	0.966	0.966	0.965	0.965	0.965	0.965	0.965	0.966	0.966	0.966
Heat capacity, C_p		Btu/lb °F	0.608	0.593	0.593	0.562	0.562	0.562	0.562	0.562	0.569	0.569	0.569
Thermal Conductivity		Btu/hr ft °F	0.031	0.028	0.028	0.022	0.022	0.022	0.022	0.022	0.023	0.023	0.023
Viscosity		cP	0.019	0.017	0.017	0.012	0.012	0.012	0.012	0.012	0.012	0.012	0.012
LIQUID PHASE													
Mass Flow Rate		lb/h		71		195							
Act. Rate		gpm		0.17		0.40							
Molecular Weight				18.015		18.015							
Density		lb/ft^3		53.132		61.274							
Heat capacity, C_p		Btu/lb °F		1.153		1.080							
Thermal Conductivity		Btu/hr ft °F		0.390		0.360							
Viscosity		cP		0.167		0.700							
Surface Tension		dyne/cm		15.517		31.608							
SOLID PHASE													
Mass Flow Rate		lb/h											
Molecular Weight													
Density		lb/ft^3											
Heat capacity, C_p		Btu/lb °F											

Table 5-3. CO_2 Reuse Pilot-Plant Process Material and Energy Balances (Streams 23-33)

Stream ID			23	24	25	26	27	28	29	30	31	32	33
Stream Description		Units	NITROGEN TO HX-202 [1]	NITROGEN TO R-200 [1]	NITROGEN TO V-202 [2]	NITROGEN TO V-304/305 [3]	FLARE GAS FROM V-304/305 [3]	CWS TO HX-100	CWR FROM HX-100	CWS TO C-100	CWR FROM C-100	CWS TO CO_2 RECOVERY UNIT	CWR FROM CO_2 RECOVERY UNIT
Temperature		°F	70.0	70.0	532.0	70.0	550.0	85.0	99.8	85.0	104.9	85.0	100.2
Pressure		psia	364.7	319.7	314.7	64.7	59.7	50.0	40.0	50.0	40.0	50.0	40.0
Molar Flow Rate		lb-mol/h	41.9	40.7	40.7	9.7	9.7	740.1	740.1	498.3	498.3	20,476.4	20,476.4
Mass Flow Rate		lb/h	1,173	1,141	1,141	272	272	13,333	13,333	8,977	8,977	368,889	368,889
Molecular Weight			28.013	28.013	28.013	28.013	28.013	18.015	18.015	18.015	18.015	18.015	18.015
HHV		Btu/scf	0.00	0.00	0.00	0.00	0.00	0.00	0.00	0.00	0.00	0.00	0.00
Fraction Vapor			1.00	1.00	1.00	1.00	1.00	0.00	0.00	0.00	0.00	0.00	0.00
TOTAL STREAM Composition	MW												
H_2O	18.015	lb-mol/h	0.000	0.000	0.000	0.000	0.000	740.113	740.113	498.317	498.317	20,476.440	20,476.442
N_2	28.013	lb-mol/h	41.880	40.716	40.716	9.710	9.710	0.000	0.000	0.000	0.000	0.000	0.000
O_2	31.999	lb-mol/h	0.000	0.000	0.000	0.000	0.000	0.000	0.000	0.000	0.000	0.000	0.000
CO_2	44.010	lb-mol/h	0.000	0.000	0.000	0.000	0.000	0.000	0.000	0.000	0.000	0.000	0.000
SO_2	64.070	lb-mol/h	0.000	0.000	0.000	0.000	0.000	0.000	0.000	0.000	0.000	0.000	0.000
H_2	2.016	lb-mol/h	0.000	0.000	0.000	0.000	0.000	0.000	0.000	0.000	0.000	0.000	0.000
CH_4	16.043	lb-mol/h	0.000	0.000	0.000	0.000	0.000	0.000	0.000	0.000	0.000	0.000	0.000
Catalyst	42.840	lb-mol/h	0.000	0.000	0.000	0.000	0.000	0.000	0.000	0.000	0.000	0.000	0.000
VAPOR PHASE													
Mass Flow Rate		lb/h	1,173	1,141	1,141	272	272						
Act. Rate		ACFM	10.77	11.96	23.12	14.19	29.41						
Std. Rate (60 °F, 14.696 psia)		MMSCFD	0.378	0.368	0.374	0.088	0.089						
Molecular Weight			28.013	28.013	28.013	28.013	28.013						
Density		lb/ft^3	1.815	1.589	0.822	0.320	0.154						
C_p/C_v			1.449	1.443	1.394	1.409	1.387						
Compressibility (Z)			0.990	0.991	1.007	0.998	1.001						
Heat capacity, C_p		Btu/lb °F	0.260	0.259	0.257	0.250	0.255						
Thermal Conductivity		Btu/hr ft °F	0.015	0.015	0.024	0.015	0.025						
Viscosity		cP	0.018	0.018	0.028	0.018	0.028						
LIQUID PHASE													
Mass Flow Rate		lb/h						13,333	13,333	8,977	8,977	368,889	368,889
Act. Rate		gpm						26.73	26.81	18.00	18.07	739.64	741.80
Molecular Weight								18.015	18.015	18.015	18.015	18.015	18.015
Density		lb/ft^3						62.181	62.007	62.181	61.939	62.181	62.002
Heat capacity, C_p		Btu/lb °F						0.998	0.998	0.996	0.996	0.998	0.998
Thermal Conductivity		Btu/hr ft °F						0.355	0.362	0.355	0.365	0.355	0.362
Viscosity		cP						0.807	0.683	0.807	0.647	0.807	0.680
Surface Tension		dyne/cm						71.279	69.970	71.279	69.509	71.279	69.938
SOLID PHASE													
Mass Flow Rate		lb/h											
Molecular Weight													
Density		lb/ft^3											
Heat capacity, C_p		Btu/lb °F											

Table 5-4. CO_2 Reuse Pilot-Plant Process Material and Energy Balances (Streams 34-44)

Stream ID			34	35	36	37	38	39	40	41	42	43	44
Stream Description		Units	CWS TO HX-300	CWR FROM HX-300	BFW TO HX-201	BFW TO V-200	BFW TO P-200/201	BFW TO HX-203	BFW/HP STEAM TO V-200	HP STEAM TO HX-204	CONDENSATE FROM HX-204	CONDENSATE FROM V-302	CONDENSATE FROM V-303
Temperature		°F	85.0	105.4	220.0	384.2	488.9	489.0	488.9	488.9	488.9	320.0	100.0
Pressure		psia	50.0	40.0	644.7	614.7	614.7	629.7	614.7	614.7	614.7	294.7	289.7
Molar Flow Rate		lb-mol/h	747.5	747.5	33.5	33.5	270.9	270.9	270.9	33.5	33.5	3.9	10.8
Mass Flow Rate		lb/h	13,466	13,466	603	603	4,881	4,881	4,881	603	603	71	195
Molecular Weight			18.015	18.015	18.015	18.015	18.015	18.015	18.015	18.015	18.015	18.015	18.015
HHV		Btu/scf	0.00	0.00	0.00	0.00	0.00	0.00	0.00	0.00	0.00	0.26	0.00
Fraction Vapor			0.00	0.00	0.00	0.00	0.00	0.00	0.15	1.00	0.00	0.00	0.00
TOTAL STREAM Composition	MW												
H_2O	18.015	lb-mol/h	747.475	747.475	33.472	33.472	270.913	270.913	270.913	33.482	33.482	3.921	10.797
N_2	28.013	lb-mol/h	0.000	0.000	0.000	0.000	0.000	0.000	0.000	0.000	0.000	0.000	0.000
O_2	31.999	lb-mol/h	0.000	0.000	0.000	0.000	0.000	0.000	0.000	0.000	0.000	0.000	0.000
CO_2	44.010	lb-mol/h	0.000	0.000	0.000	0.000	0.000	0.000	0.000	0.000	0.000	0.000	0.000
SO_2	64.070	lb-mol/h	0.000	0.000	0.000	0.000	0.000	0.000	0.000	0.000	0.000	0.000	0.000
H_2	2.016	lb-mol/h	0.000	0.000	0.000	0.000	0.000	0.000	0.000	0.000	0.000	0.000	0.000
CH_4	16.043	lb-mol/h	0.000	0.000	0.000	0.000	0.000	0.000	0.000	0.000	0.000	0.001	0.000
Catalyst	42.840	lb-mol/h	0.000	0.000	0.000	0.000	0.000	0.000	0.000	0.000	0.000	0.000	0.000
VAPOR PHASE													
Mass Flow Rate		lb/h							734	603			
Act. Rate		ACFM							9.19	7.55			
Std. Rate (60 °F, 14.696 psia)		MMSCFD							0.303	0.249			
Molecular Weight									18.015	18.015			
Density		lb/ft^3							1.332	1.332			
C_p/C_v									3.054	3.054			
Compressibility (Z)									0.817	0.817			
Heat capacity, C_p		Btu/lb °F							0.922	0.922			
Thermal Conductivity		Btu/hr ft °F							0.030	0.030			
Viscosity		cP							0.018	0.018			
LIQUID PHASE													
Mass Flow Rate		lb/h	13,466	13,466	603	603	4,881	4,881	4,146		603	71	195
Act. Rate		gpm	27.00	27.11	1.26	1.38	12.28	12.29	10.44		1.52	0.17	0.40
Molecular Weight			18.015	18.015	18.015	18.015	18.015	18.015	18.015		18.015	18.015	18.015
Density		lb/ft^3	62.181	61.932	59.743	54.423	49.534	49.533	49.534		49.534	53.132	61.274
Heat capacity, C_p		Btu/lb °F	0.996	0.996	1.004	1.065	1.172	1.173	1.172		1.172	1.153	1.080
Thermal Conductivity		Btu/hr ft °F	0.355	0.365	0.394	0.386	0.356	0.356	0.356		0.356	0.390	0.360
Viscosity		cP	0.807	0.644	0.270	0.138	0.104	0.104	0.104		0.104	0.167	0.700
Surface Tension		dyne/cm	71.279	69.463	58.047	38.654	25.138	25.117	25.138		25.138	15.517	31.608
SOLID PHASE													
Mass Flow Rate		lb/h											
Molecular Weight													
Density		lb/ft^3											
Heat capacity, C_p		Btu/lb °F											

Table 5-5. CO_2 Reuse Pilot-Plant Process Material and Energy Balances (Streams 41-47)

Stream ID			41	42	43	44	45	46	47
Stream Description		Units	HP STEAM TO HX-204	CONDENSATE FROM HX-204	CONDENSATE FROM V-302	CONDENSATE FROM V-303	CONDENSATE FROM V-302 & V-303	CONDENSATE FROM V-100	LP STEAM TO CO_2 RECOVERY
Temperature		°F	488.9	488.9	320.0	100.0	121.2	91.4	297.7
Pressure		psia	614.7	614.7	294.7	289.7	289.7	21.8	64.7
Molar Flow Rate		lb-mol/h	33.5	33.5	3.9	10.8	14.7	7.6	341.0
Mass Flow Rate		lb/h	603	603	71	195	265	140	6,144
Molecular Weight			18.015	18.015	18.015	18.015	18.015	18.551	18.015
HHV		Btu/scf	0.00	0.00	0.26	0.00	0.07	0.00	0.00
Fraction Vapor			1.00	0.00	0.00	0.00	0.00	0.00	1.00
TOTAL STREAM Composition	MW								
H_2O	18.015	lb-mol/h	33.482	33.482	3.921	10.797	14.718	7.397	383.647
N_2	28.013	lb-mol/h	0.000	0.000	0.000	0.000	0.000	0.012	0.000
O_2	31.999	lb-mol/h	0.000	0.000	0.000	0.000	0.000	0.001	0.000
CO_2	44.010	lb-mol/h	0.000	0.000	0.000	0.000	0.000	0.150	0.000
SO_2	64.070	lb-mol/h	0.000	0.000	0.000	0.000	0.000	0.000	0.000
H_2	2.016	lb-mol/h	0.000	0.000	0.000	0.000	0.000	0.000	0.000
CH_4	16.043	lb-mol/h	0.000	0.000	0.001	0.000	0.001	0.000	0.000
Catalyst	42.840	lb-mol/h	0.000	0.000	0.000	0.000	0.000	0.000	0.000
VAPOR PHASE									
Mass Flow Rate		lb/h	603						6,144
Act. Rate		ACFM	7.55						684.42
Std. Rate (60 °F, 14.696 psia)		MMSCFD	0.249						2.977
Molecular Weight			18.015						18.015
Density		lb/ft^3	1.332						0.150
C_p/C_v			3.054						1.274
Compressibility (Z)			0.817						0.959
Heat capacity, C_p		Btu/lb °F	0.922						0.541
Thermal Conductivity		Btu/hr ft °F	0.030						0.018
Viscosity		cP	0.018						0.014
LIQUID PHASE									
Mass Flow Rate		lb/h		603	71	195	265	140	
Act. Rate		gpm		1.52	0.17	0.40	0.54	0.30	
Molecular Weight				18.015	18.015	18.015	18.015	18.551	
Density		lb/ft^3		49.534	53.132	61.274	61.748	58.715	
Heat capacity, C_p		Btu/lb °F		1.172	1.153	1.080	0.996	0.958	
Thermal Conductivity		Btu/hr ft °F		0.356	0.390	0.360	0.372	0.161	
Viscosity		cP		0.104	0.167	0.700	0.551	0.634	
Surface Tension		dyne/cm		25.138	15.517	31.608	68.014	69.703	
SOLID PHASE									
Mass Flow Rate		lb/h							
Molecular Weight									
Density		lb/ft^3							
Heat capacity, C_p		Btu/lb °F							

Table 5-6. Gas Properties of Streams 1 and 3

Stream Property	Stream 1	Stream 3
Flow rate (SCFM)	211.05	47.68
Composition (mole fraction)		
H_2	0.898	0.000
CO_2	0.000	1.000
CH_4	0.102	0.000
CO	0.000	0.000
H_2O	0.000	0.000
Total	1.000	1.000
Temperature (°C)	38 (100°F)	38 (100°F)
Pressure (psia)	14.7	14.7

SCFM = Standard cubic feet per minute

After entering the transport reactor R-200, the fuel gas flowed upward through a fluidized bed consisting of Ni-based catalyst, where the fuel gas acted as the fluidization medium. In the presence of the catalyst, the CO_2 and H_2 in the fuel gas reacted to produce CH_4 and H_2O via the reaction in Equation 1. The reaction converted 98.4% of H_2 and 96.8% of CO_2 into 119 lb/h of CH_4 and 267 lb/h of H_2O. This reaction required a minimum of 26,626 lb/h of Ni-based catalyst (Stream 8) circulating through R-200. This exothermic reaction generated a heat load of 538,012 Btu/h. The reactor R-200 was not designed with heat transfer internals, but the solid catalyst particles absorbed the heat generated by the exothermic reaction and effectively moderated the temperature rise. The temperature of the stream exiting the reactor (Stream 7) was 300 °C (572 °F).

Because Stream 7 contained both gas and hot circulating solids, a cyclone (V-201) was used to separate the solid catalyst particles from the gas. The hot solids were then fed to a solids cooler (HX-203) to reduce the solids temperature to 250 °C (482 °F). The solids cooler exchanged heat with high-pressure boiler feed water to produce 603 lb/h of high-pressure steam (Stream 41). The hot gas from the cyclone (Stream 10) flowed through a filter (F-200/201) to remove any remaining catalyst before entering the feed gas heater (HX-200) to reduce its temperature to 215 °C (419 °F). Finally, this reactor off-gas was further cooled in the boiler feed water heater (HX-201) to the point where appreciable condensation occurred. This exchanger cooled the gas to 160 °C (320 °F) while heating 603 lb/h of high-pressure boiler feed water to 196 °C (384 °F). The flow rate, composition, and other stream properties of the reactor off-gas exiting HX-201 (Stream 13) are shown in Table 5-7.

Table 5-7. Properties of Reactor Off-Gas Stream 13

Stream Property	Value
Flow rate (lb/h)	637
Composition (mole fraction)	
H_2	0.019
CO_2	0.009
CH_4	0.581
CO	0.000
H_2O	0.390
Total	0.999
Temperature (°C)	160 (320 °F)
Pressure (psia)	294.7
Vapor fraction	0.90

Boiler feed water (Stream 36) entered the process at a flow rate of 603 lb/h, a temperature of 104 °C (220 °F), and a pressure of 644.7 psia. This stream was heated in the boiler feed water heater (HX-201) to a temperature of 196 °C (384 °F). The boiler feed water effluent (Stream 37) entered the steam drum (V-200), where it was mixed with the hot stream from the solids cooler (HX-203). The steam drum separated the liquid from the vapor of this mixed stream. The liquid from the steam drum was then sent to HX-203 to be partially vaporized. The steam emitted from the steam drum had two possible destinations. First, the steam was condensed in an air cooler (HX-204) to produce 603 lb/h of condensate (Stream 42). Second, the steam was combined with 14 lb/h of boiler feed water in the desuperheater (HX-101) to produce 617 lb/hr of low-pressure steam for use in the CO_2 recovery unit.

The two-phase reactor off-gas exiting HX-201 (Stream 13) was sent to knockout (KO) drum #2 (V-302), where 71 lb/h of condensed water (Stream 43) was separated from the remaining gas. The resultant gas stream (Stream 14) entered the trim cooler (HX-300) to reduce its temperature to 38 °C (100 °F) by exchanging heat with cooling water. The cooling water entered the exchanger at 30 °C (85 °F) as Stream 34 and exited at 41 °C (105 °F) as Stream 35. The cooled gas (Stream 15) then flowed to KO drum #3 (V-303), where 195 lb/h of condensed water (Stream 44) was separated from it. To remove any remaining H_2O, the gas was then sent to a molecular-sieve dryer (V-304/305), which removed 1 lb/h of H_2O. The molecular sieve used in the dryer was Zeolite 4A, a commonly used drying agent for natural gas streams. The flow rate of the final SNG product (Stream 18) was 182 lb/h. Its composition, temperature, and pressure are presented in Table 5-8.

Table 5-8. Properties of Product SNG Stream 18

Stream Property	Value
Flow rate (SCFM)	69.21
Composition (mole fraction)	
H_2	0.031
CO_2	0.016
CH_4	0.953
CO	0.000
H_2O	0.000
Total	1.000
Temperature (°C)	38 (100 °F)
Pressure (psia)	289.7

SCFM = Standard cubic feet per minute

5.1.1 Vessel and Equipment Descriptions

B-100

Flue-Gas Blower

Description: The blower B-100 was used to elevate the inlet flue-gas pressure for the CO_2 recovery unit from atmospheric pressure to 21.8 psia. The flue gas was sent to the CO_2 recovery unit to capture the CO_2 that would be used by the CO_2 reuse process unit to produce SNG.

Design Basis:

- Capacity: 28,176 actual cubic feet per hour (ft^3/h; gas flow)
- Differential pressure: 7.1 pounds per square inch (psi)
- Work power: 23 horsepower (HP; 75% efficiency)
- Type: Centrifugal
- Material: Carbon steel
- Inlet and outlet process stream composition, temperature, and pressure (see Material Balance)

C-100

Fuel-Gas Compressor

Description: The compressor C-100 was used to compress the combined stream of fuel gas (Stream 1) and CO_2 (Stream 3) after mixing from 14.7 to 319.7 psia to the reaction pressure in transport reactor R-200 and to overcome pressure losses throughout the process. The C-100 compressor consisted of four stages with intercoolers fed with cooling water (Stream 30). This cooling water was returned back to the plant (Stream 31).

Design Basis:

- Capacity: 18,385 actual ft^3/h (gas flow)
- Cooling water capacity: 20 gallons per minute [gpm; 29 °C (85 °F) supply and 41 °C (105 °F) return]
- Differential pressure: 305 psi
- Work power: 132 HP (78% efficiency)
- Type: Four-stage centrifugal
- Material: Carbon steel
- Inlet and outlet process stream composition, temperature, and pressure (see Material Balance)

C-300

SNG Recycle Compressor

Description: Stream 17 was split into a product SNG stream (Stream 18) and a recycle SNG stream (Stream 19). The recycle SNG was used as fluidizing gas in the reactor J-leg and the solids cooler (HX-203). To overcome pressure losses in the reactor J-leg and the solids cooler, the pressure of the fluidizing gas Stream 19 was raised using compressor C-300 from 289.7 to 319.7 psia. The C-300 compressor consisted of one stage and did not require any cooling water.

Design Basis:

- Capacity: 259 actual ft^3/h (gas flow)
- Differential pressure: 30 psi
- Work power: 0.9 HP (78% efficiency)
- Type: One-stage centrifugal
- Material: Carbon steel
- Inlet and outlet process stream composition, temperature, and pressure (see Material Balance)

CO_2 RECOVERY UNIT

CO_2 Recovery Unit

Description: The CO_2 from the flue gas (Stream 2) was captured in a CO_2 recovery unit using 30 wt% monoethanolamine (MEA) as the absorbing solvent. The captured CO_2 was sent to the CO_2 reuse process unit as Stream 3, and the treated flue gas was returned to the plant.

Design Basis:

- Capacity: 4.5 tons/day of CO_2 captured
- Material: Carbon steel
- Inlet and outlet process stream composition, temperature, and pressure (see Material Balance)

F-200/201

Filter (Two Filters, One Spare)

Description: Sintered-metal filter F-200/201 was used to remove 99.9% of all solids in Stream 10, the gas stream leaving the cyclone V-201. The attrition rate of solids to the filter was assumed to be 100 lb/MMlb circulated.

Design Basis:

- Type: Porous sintered-metal hot-gas filter
- Area: 3.175 square feet (ft^2)
- Space velocity: 7 feet per minute (ft/min; Mott)
- Gas flow: 1,467 actual ft^3/h (gas flow)
- Solids flow: 2.6 lb/h
- Material: 304 SS
- Inlet and outlet process stream composition, temperature, and pressure (see Material Balance)

HX-100

Flue-Gas Cooler

Description: The pressurized flue gas exiting flue-gas blower B-100 was cooled to 38 °C (100 °F) in condenser HX-100 (flue-gas cooler) with cooling water (Stream 28). The resulting cooled gas then entered KO drum #1 (V-100), where the condensed water in the stream was removed. The used cooling water from HX-100 was returned to the plant as Stream 29.

Design Basis:

- Capacity: 21,937 actual ft^3/h (gas flow)
- Cooling water demand: 30 gpm [29 °C (85 °F) supply and 38 °C (100 °F) return]
- Type: Gas-liquid shell-and-tube heat exchanger
- Area: 221.87 ft^2
- Overall heat transfer coefficient: 25 $Btu/(h \cdot ft^2 \cdot °R)$
- Log mean temperature differential (LMTD): 40.04 °F
- Heat duty: 221,315 Btu/h
- Material: Carbon steel
- Inlet and outlet process stream composition, temperature, and pressure (see Material Balance)

HX-101

Desuperheater

Description: Desuperheater HX-101 was used to depressurize high-pressure steam to low-pressure steam by using boiler feed water. The pressure of the resulting low-pressure steam was 64.7 psia.

Design Basis:

- Capacity: 663 lb/h (high-pressure steam flow)
- Boiler feed water flow: 15 lb/h [104 °C (220 °F), 644.7 psia]
- Steam pressure drop: 550 psi
- Material: Carbon steel
- Inlet and outlet process stream composition, temperature, and pressure (see Material Balance)

HX-200

Feed-Gas Heater

Description: The off-gas (Stream 11) from the filter F-200/201 was used to heat the reactor gas feed (Stream 5) in heat exchanger HX-200 (feed-gas heater). The fuel gas was elevated to the required reaction temperature of 250 °C (482 °F) before entering transport reactor R-200 as Stream 6.

Design Basis:

- Capacity: 1,150 actual ft^3/h (fuel-gas flow) and 1,467 actual ft^3/h (reactor off-gas flow)
- Type: Gas-gas shell-and-tube heat exchanger
- Area: 21.60 ft^2
- Overall heat transfer coefficient: 30 $Btu/(h \cdot ft^2 \cdot °R)$
- LMTD: 105.30 °F

- Heat duty: 66,990 Btu/h
- Material: Carbon steel
- Inlet and outlet process stream composition, temperature, and pressure (see Material Balance)

HX-201

Boiler Feed Water Heater

Description: The reactor off-gas exiting feed gas heater HX-200 (Stream 12) was used to preheat boiler feed water (Stream 36) in heat exchanger HX-201 (boiler feed water heater). The preheated boiler feed water (Stream 37) then entered the steam drum V-200, while the reactor off-gas exited HX-201 (Stream 13) and proceeded to the condenser area. The purpose of heating the boiler feed water was to bring its temperature close to the saturation temperature for high-pressure steam. The heated boiler feed water was then partially vaporized in the solids cooler (HX-203) to aid in cooling the solid catalyst.

Design Basis:

- Capacity: 663 lb/h (boiler feed water mass flow) and 1,275 actual ft^3/h (reactor off-gas flow)
- Type: Gas-liquid shell-and-tube heat exchanger
- Area: 73.04 ft^2
- Overall heat transfer coefficient: 25 $Btu/(h \cdot ft^2 \cdot °R)$
- LMTD: 16.5 °C (61.7 °F)
- Heat duty: 111,994 Btu/h
- Material: Carbon steel
- Inlet and outlet process stream composition, temperature, and pressure (see Material Balance)

HX-202

Start-Up Heater

Description: An electric circulation heater (HX-202) was used to heat N_2 that was used during start-up to preheat the reactor system. After the reactor was heated, the flow of fuel-gas Stream 5 through HX-200 was then started.

Design Basis:

- Power input: 128 kilowatts (kW)
- Type: Electric circulation heater
- Material: Carbon steel shell with Incoloy internal elements
- Inlet and outlet process stream composition, temperature, and pressure (see Material Balance)

HX-203

Solids Cooler

Description: The solids cooler was used to cool the hot solids exiting cyclone V-201 (Stream 8) before they were returned as Stream 9 to the reactor. The hot solids partially vaporized the boiler feed water (Stream 39) to produce saturated, high-pressure steam (Stream 40). The solids cooler was a bayonet heat exchanger in which the boiler feed water flowed through multiple U-shaped tubes and the solids passed along the outside of these tubes. To ensure that the solids sufficiently contacted the tubes, a portion of the product SNG leaving the molecular-sieve dryer (V-304/305) was recycled to fluidize the solid catalyst. The solids in the J-leg return to the reactor (Stream 9) were also fluidized by the recycled SNG.

Design Basis:

- Type: Bayonet heat exchanger
- Material: 304 SS
- Area: 311.02 ft^2

- Heat duty: 591,813 Btu/h
- Boiler feed water flow: 663 lb/h
- Solids flow: 29,289 lb/h
- Fluidization velocity: 0.03 feet per second (ft/s)
- LMTD: 19.0 °F
- Overall heat transfer coefficient: 100 Btu/(h·ft^2·°R)
- Inlet and outlet process stream composition, temperature, and pressure (see Material Balance)

HX-204

Air Cooler

Description: The high-pressure steam exiting steam drum V-200 (Stream 41) either entered the air-cooled fin cooler (HX-204) to condense it to boiler feed water for return to the plant or was combined with boiler feed water in the desuperheater (HX-101) to produce low-pressure steam for use in the CO_2 recovery unit. The air cooler HX-204 consisted of a fan with motor that blew air over a finned tube bank to condense the steam (Stream 42).

Design Basis:

- Steam Flow: 663 lb/h
- Type: Air-cooled heat exchanger
- Area: 9.82 ft^2
- Overall heat transfer coefficient: 135 Btu/(h·ft^2·°R)
- LMTD: 186.0 °C (366.79 °F)
- Heat duty: 483,392 Btu/h
- Power input: 6 kW
- Material: Carbon steel
- Inlet and outlet process stream composition, temperature, and pressure (see Material Balance)

HX-300

Trim Cooler

Description: The reactor off-gas (Stream 14) exiting KO drum #2 (V-302) was cooled to 38 °C (100 °F) in condenser HX-300 (trim cooler) using cooling water (Stream 34). The resulting cooled gas (Stream 15) then entered KO drum #3 (V-303) to separate any condensed water from the gas. The used cooling water from HX-300 was returned to the plant as Stream 35.

Design Basis:

- Capacity: 1,025 actual ft^3/h (off-gas flow)
- Cooling water demand: 30 gpm (85 °F supply and 105 °F return)
- Type: Gas-liquid shell-and-tube heat exchanger
- Area: 161.40 ft^2
- Overall heat transfer coefficient: 25 Btu/(h·ft^2·°R)
- LMTD: 23.9 °C (75.0 °F)
- Heat duty: 301,382 Btu/h
- Material: Carbon steel
- Inlet and outlet process stream composition, temperature, and pressure (see Material Balance)

HX-301

N_2 Heater

Description: An electric circulation heater HX-301 (N_2 heater) was used to heat the nitrogen (Stream 26) used to regenerate the Zeolite 4A molecular-sieve dryers (V-304/305). To desorb the H_2O from the zeolite, the nitrogen was heated to 288 °C (550 °F). After a 24-hour desorption period, the heater

was turned off while the nitrogen continued to flow through the molecular-sieve dryers for another 6 hours to cool the dryers to ambient temperature.

Design Basis:

- Power input: 32 kW
- Type: Electric circulation heater
- Material: Carbon steel shell with Incoloy internal elements
- Inlet and outlet process stream composition, temperature, and pressure (see Material Balance)

P-200/201

Boiler Feed Water Pump (Two Pumps, One Spare)

Description: A boiler feed water pump (P-200/201) was used to provide the pressure needed to pump the H_2O from the steam drum V-200 to the solids cooler HX-203, which was located at a higher elevation (i.e., Streams 38 and 39).

Design Basis:

- Capacity: 14 gpm
- Total dynamic head (TDH): 160 feet (ft.)
- Pressure differential: 15 psi
- Power input: 2.19 brake horsepower (BHP)
- Type: Centrifugal
- Material: Carbon steel
- Inlet and outlet process stream composition, temperature, and pressure (see Material Balance)

R-200

Transport Reactor Methanator

Description: The fuel gas (Stream 6) containing H_2 and CO_2 was mixed with the Ni-based catalyst particles in the transport reactor R-200, where the reactants reacted to produce CH_4 and H_2O. This R-200 reactor was a fluidized bed, with the fuel gas acting as the fluidizing medium. Though the methanation reaction was exothermic (reaction in Equation 1), the solid catalyst particles absorbed the majority of the reaction heat, effectively moderating the heat released. The off-gas and hot catalyst particles were separated in the cyclone V-201. The off-gas was further processed downstream into product SNG, while the solids were cooled in the solids cooler HX-203 before being returned to the reactor. The R-200 reactor system consisted of a mixing zone, riser, cyclone, standpipe, J-leg, and solids cooler. The fuel-gas feed was introduced at the bottom of the mixing zone and then traveled up through the riser. The reaction producing CH_4 and H_2O occurred in the mixing zone and riser. The pipe connecting the riser to the cyclone was sloped downward at 15 degrees to help solids flow into the cyclone. The solid catalyst was separated from the gas in the cyclone and passed through the standpipe to reach the solids cooler. After passing through the solids cooler, the solids were returned to the reactor mixing zone by way of the J-leg section. This J-leg section was fluidized by recycled SNG flowing at a velocity of 0.5 ft/s.

Design Basis:

- Capacity: 1,455 actual ft^3/h (fuel-gas flow); 1,176 ft^3/h (off-gas flow); and 29,289 lb/h (solid-catalyst circulation rate)
- Gas velocity: 2.49 ft/s in mixing zone and 9.95 ft/s in riser
- Type: Vertical pressure vessel
- Total height: 100 ft. (20 ft. for mixing zone; 60 ft. for riser; 20 ft. off grade for mixing zone)
- Inside diameter: 6 in. for mixing zone; 3 in. for riser, 6 in. for standpipe; and 3 in. for J-leg
- Fluidization velocity: 0.5 ft/s
- Material: 304 SS

- Refractory thickness: 2 in.
- Inlet and outlet process stream composition, temperature, and pressure (see Material Balance)

V-100
KO Drum #1

Description: The KO drum #1 (V-100) was used to separate the condensed water from the cooled flue gas exiting the flue-gas cooler HX-100. The condensate left as Stream 46 from the bottom of the V-100 vessel, while the gas exited from the top of the vessel and proceeded to the CO_2 recovery unit.

Design Basis:

- Capacity: 15,336 actual ft^3/h (inlet flow); 15,333 actual ft^3/h (outlet gas flow); and 158 lb/h (condensate mass flow)
- Type: Vertical pressure vessel
- T/T: 5.5 ft.
- Diameter: 18 in. nominal pipe size (NPS; Schedule 40)
- Material: Carbon steel
- Inlet and outlet process stream composition, temperature, and pressure (see Material Balance)

V-200
Steam Drum

Description: The preheated boiler feed water (Stream 37) entered the steam drum V-200 and then exited through the downcomer pipe as Stream 38 before entering the solids cooler HX-203. In the solids cooler, this boiler feed water absorbed the heat from the solids, partially vaporizing in the process, before returning as Stream 40 to the steam drum, where this now saturated steam was separated into steam and H_2O. The steam then exited the top of the drum as Stream 41 before passing through the air-cooled exchanger HX-204.

Design Basis:

- Capacity: 663 lb/h (boiler feed water mass flow) and 5,369 lb/h (partially vaporized steam mass flow)
- Type: Vertical pressure vessel
- T/T: 9.5 ft.
- Diameter: 36 in. NPS (Schedule 40)
- Material: Carbon steel
- Inlet and outlet process stream composition, temperature, and pressure (see Material Balance)

V-201
Cyclone

Description: After exiting the transport reactor R-200, the hot catalyst solids and off-gas were sent into a cyclone (V-201) to separate the solids from the gas. The solids exited the bottom of the cyclone as Stream 8 and proceeded to the solids cooler HX-203. The off-gas, leaving from the top of the cyclone as Stream 10, proceeded to the filter F-200/201.

Design Basis:

- Capacity: 1,467 actual ft^3/h (reactor off-gas flow) and 29,289 lb/h (solids mass flow)
- Diameter: 24 in. NPS (Schedule 40)
- Type: Pressure vessel
- Material: Carbon steel
- Inlet and outlet process stream composition, temperature, and pressure (see Material Balance)

V-202

Catalyst Hopper

Description: Although the solid catalyst was separated from the off-gas stream in cyclone V-201, some solids still flowed through the cyclone with the off-gas and were hence lost from the reactor system. To replenish the reactor system with fresh catalyst, a lock hopper system (V-202) with Everlast valves was designed based on an assumed solids attrition rate of 100 lb/MMlb circulated.

Design Basis:

- Material: 304 SS
- Lock hopper size: 30-day total supply; V-202 with refill after 21 days; 2,372 lb.; 4 ft. hopper height; 4 ft. cone height; and 3 ft. diameter

V-302

KO Drum #2

Description: A KO drum #2 (V-302) was used to separate the condensate from the off-gas Stream 13 exiting HX-201. The condensate left from the bottom of the vessel as Stream 43, while the gas exited from the top of the vessel as Stream 14 and proceeded to the off-gas condenser HX-300 (trim cooler) for further cooling before entering KO drum #3 (V-303).

Design Basis:

- Capacity: 1,026 actual ft^3/h (inlet flow); 1,025 actual ft^3/h (outlet gas flow); and 78 lb/h (condensate mass flow)
- Type: Vertical pressure vessel
- T/T: 5.0 ft.
- Diameter: 18 in. NPS (Schedule 40)
- Material: Carbon steel
- Inlet and outlet process stream composition, temperature, and pressure (see Material Balance)

V-303

KO Drum #3

Description: A KO drum #3 (V-303) was used to separate the condensate from the cooled off-gas Stream 15 exiting the trim cooler HX-300. The condensate exited from the bottom of the vessel as Stream 44, while the gas left from the top of the vessel as Stream 16 and proceeded to the molecular-sieve dryer (V-304/305) for removal of the remaining H_2O.

Design Basis:

- Capacity: 514 actual ft^3/h (inlet flow), 510 actual ft^3/h (outlet gas flow), 215 lb/h (condensate mass flow)
- Type: Vertical pressure vessel
- T/T: 5.5 ft.
- Diameter: 18 in. NPS (Schedule 40)
- Material: Carbon steel
- Inlet and outlet process stream composition, temperature, and pressure (see Material Balance)

V-304/305

Molecular-Sieve Dryer (Two Vessels, One Spare)

Description: For final drying, the off-gas Stream 16 exiting KO drum #3 (V-303) was sent to one of the molecular-sieve dryer vessels V-304 or V-305, depending on which vessel was being operated at the time. These vessels contained a bed of Zeolite 4A material for adsorbing the H_2O from the gas. The resulting dried off-gas then exited from the top of the V-303 vessel as product SNG (Stream 17). Water adsorbed on the zeolite beds was desorbed by first flowing heated nitrogen over the bed for 24

hours and then letting the bed cool for 6 hours under flowing unheated nitrogen. The nitrogen containing the desorbed H_2O exited from the top of vessel V-303 as Stream 27 and was sent to the flare.

Design Basis:

- Capacity: 510 actual ft^3/h (inlet gas flow), 509 actual ft^3/h (outlet gas flow), 62.60 standard ft^3/min (nitrogen gas flow), and 1.4 lb/h (water mass adsorbed)
- Type: Vertical pressure vessel
- T/T: 7.5 ft.
- Diameter: 2.5 ft.ID (inner diameter)
- Material: Carbon steel
- Inlet and outlet process stream composition, temperature, and pressure (see Material Balance)

6. Preliminary Cost Estimation

With information on the materials of construction, operating and design temperatures and pressures, heat duties and major equipment power requirements from the preliminary engineering package in Section 5, the web site <http://matche.com> was used to develop cost estimates for a majority of the equipment for the pilot demonstration unit for the CO_2 reuse process. This web site, which gives cost estimates for a wide variety of equipment, only provides the uninstalled cost for each type of equipment. All equipment costs on this web site are based on 2007 pricing in U.S. dollars. To determine the equipment cost in 2010, a 3% per year inflation rate was added to the cost obtained from this web site. Some of the equipment was also estimated from vendor quotations obtained for previous projects and/or proposals. The total uninstalled equipment cost for the pilot demonstration unit for RTI's CO_2 reuse process was estimated to be $1,953,090, as shown in Table 6-1.

The installed equipment cost for the pilot demonstration unit for RTI's CO_2 reuse process was estimated to be $5,859,271, which included labor, structure and balance of plant, insulation, transportation, piping, and electrical components. The method used to determine this installed cost was the Lang Method, which estimates installed costs to be three times the uninstalled costs.

Assuming an estimated catalyst cost of $30 per pound, the cost for the catalyst was $156,630. Using typical commercial pricing for molecular sieves, the estimated cost for this adsorbent was $101,580.

By summing the uninstalled equipment costs, the installed equipment costs, and the catalyst and adsorbent costs, the preliminary total installed cost for the pilot demonstration unit for RTI's CO_2 reuse process was estimated to be $8,070,332. Table 6-1 summarizes the development of this preliminary cost estimate and includes all major equipment and the key design criteria used to estimate this cost.

Table 6-1. Equipment List and Preliminary Cost for RTI's CO_2 Reuse Process

PROJECT NAME: CO_2 REUSE PROJECT NUMBER: 0212476 DATE: 4/27/10 By: WJY, Chkd By: SPR, Appr. By: AJ REV. 0	RTI International Center for Energy Technology 3040 E. Cornwallis Rd. PO Box 12194 RTP, NC 27709-2194 USA				EQUIPMENT LIST & COST ESTIMATE SUMMARY				
TAG NUMBER	DESCRIPTION	TYPE	SIZE	WEIGHT	OPERATING TEMPERATURE	OPERATING PRESSURE	MATERIALS	PRICE, TOTAL (uninstalled)	REFERENCE
B-100	Flue Gas Blower	Centrifugal	23 HP, 470 acfm, 75% efficiency	n/a	225 °F	22 PSIA	300#, Carbon Steel	$ 79,031	(1)
CO_2 Recovery Unit	CO_2 Recovery Unit		4.5 ton/day CO_2 captured					$ 437,500	
C-100	Fuel Gas Compressor	centrifugal	132 HP, 78% efficiency	n/a	296 °F	320 PSIA	300#, Carbon Steel	$ 247,871	Engineering Estimate
C-300	SNG Recycle Compressor	Centrifugal	0.89 HP, 78% efficiency	n/a	100 °F	315 PSIA	300#, Carbon Steel	$ 12,481	Engineering Estimate
F-200/201	Process Gas Filter	sintered metal	3.175 ft^2	n/a	572 °F	310 PSIA	300#, 304SS	$ 41,210	(1), assumed 7ft/min face velocity
HX-100	Flue Gas Cooler	shell & tube	221.87 ft^2	n/a	225 °F	50 PSIA	150 #, Carbon Steel	$ 19,669	(1)
HX-101	Desuperheater			n/a	489 °F	615 PSIA	600#, Carbon Steel	$ 5,000	Engineering Estimate
HX-200	Feed Gas Heater	shell & tube	21.60 ft^2	n/a	572 °F	320 PSIA	300#, Carbon Steel	$ 8,633	(1)
HX-201	BFW Heater	shell & tube	73.04 ft^2	n/a	364 °F	645 PSIA	600#, Carbon Steel	$ 16,391	(1)
HX-202	Start-up Heater	circulation	128 kW	n/a	482 °F	14.7 PSIA	300#, Carbon Steel shell/Incoloy elements	$ 168,960	estimated from Chromalox quotation
HX-203	Solids Cooler	shell & tube	311.02 ft^2	n/a	350 °F	615 PSIA	600#, 304SS	$ 476,757	(1)
HX-204	Air Cooler with Fan	fin tube	9.82 ft^2	n/a	489 °F	615 PSIA	600#, Carbon Steel	$ 37,808	(1)
HX-300	Trim Cooler	shell & tube	161.40 ft^2	n/a	482 °F	305 PSIA	300#, Carbon Steel	$ 18,904	(1)
HX-301	N_2 Heater	circulation	32 kW	n/a	550 °F	64.7 PSIA	150#, Carbon Steel shell/Incoloy elements	$ 42,240	Chromalox quotation
P-200/201	BFW pump	centrifugal	2.19 BHP, 14 GPM, 160 ft TDH	n/a	489 °F	615 PSIA	600#, Carbon Steel	$10,000	1 op, 1 spare, based on STC provided quotation
R-200	Transport Reactor	transport		8,301 lbs steel, 1,876 lbs SiCarbide refractory	482 °F	315 PSIA	300#, 304SS	$ 111,214	(1), '(3), '(4)
V-100	KO Drum #1	vertical	5.5' T/T x 18" NPS	1,747 lbs	91 °F	22 PSIA	150#, Carbon Steel	$ 21,964	(1)
V-200	Steam Drum	vertical	9.5' T/T x 36" NPS, 2" wall	9,062 lbs	489 °F	615 PSIA	600#, Carbon Steel	$ 48,299	(1)
V-201	Cyclone	cyclone	24" NPS, 22 ACFM	656 lbs	482 °F	315 PSIA	300#, 304SS	$ 24,096	(1)
V-202	Catalyst Hopper			2,146 lbs			300#, Carbon Steel	$ 34,696	(1)
V-302	KO Drum #2	vertical	5' T/T x 18" NPS	1,735 lbs	320 °F	295 PSIA	300#, Carbon Steel	$ 21,964	(1)
V-303	KO Drum #3	vertical	5.5' T/T x 18" NPS	1,787 lbs	100 °F	290 PSIA	300#, Carbon Steel	$ 22,292	(1)
V-304/305	Mol. Sieve Dryer	packed bed/vertical	7.5' T/T x 2.5' ID, 2.00" wall	1,907 lbs	100 °F	290 PSIA	300#, Carbon Steel	$ 46,113	(1)
Total Uninstalled Equipment Cost								$ 1,953,090	
Installed Cost (Labor, Structural, Piping, Insulation etc.)								$ 5,859,271	(2)
Catalyst Cost								$ 156,390	(5)
Adsorbent Cost (for 2 vessels)								$ 101,580	(5)
Total Installed Cost								**$ 8,070,332**	
(1) cost estimate from matche.com									
(2) Lang Method states that installation costs are 3 times equipment material costs									
(3) http://www.insulation.org/articles/article.cfm?id=IO021001									
(4) http://www.answers.com/topic/silicon									
(5) Assumed $30/lb of catalyst and adsorbent									

7. Conclusions and Recommendations

This Phase I research investigated the feasibility of converting CO_2 into pipeline-quality SNG by using a transport reactor-based methanation process. Using methanation activity and selectivity criteria developed on the basis of commercial fixed-bed methanation catalysts, various catalyst synthesis/preparation techniques were used to develop, prepare, and optimize two fluidizable Ni-based catalyst formulations, Cat-1 and Cat-3, with high methanation activity and selectivity under fluidized-bed conditions. Furthermore, both the Cat-1 and Cat-3 formulations were successfully scaled up using commercial manufacturing equipment. Process feasibility was demonstrated in a pilot transport reactor with the scaled batch of Cat-1. Using information acquired from bench- and pilot-scale testing, a basic engineering design (BED) package and preliminary cost estimate for a 4-ton/day CO_2 pilot demonstration unit were prepared.

Significant accomplishments and major conclusions of this study are:

- Development of BED package for a pilot demonstration unit for RTI's CO_2 reuse process, including PFD, material and energy balances, PIDs, equipment list, interface diagrams, plot plan, and preliminary cost estimate
- Evaluation of methanation activity of five commercial methanation catalyst formulations under fluidized-bed conditions
- Development of two catalysts formulations, Cat-1 and Cat-3, for fluidized-bed applications. These formulations were shown to possess similar or better methanation performance than commercial catalysts.
- Investigation of two synthesis methods (constant pH and raised pH) using various precipitation agents
- Determining that precipitating agent significantly affected catalyst performance
- Little to no degradation in Cat-1 methanation activity after extended bench-scale testing (800 hours)
- Successful scale-up of 100-lb batch of Cat-1 at SCI's pilot-plant facility in Louisville, KY, for pilot-plant testing. During bench-scale testing, it was demonstrated that the scaled material calcined at 350 °C had methanation activity and selectivity essentially identical to that of the corresponding laboratory-prepared material.
- Successful demonstration of process feasibility during pilot transport reactor testing at KBR's Technology Center in Houston, TX. Pilot-scale testing with the scaled batch of Cat-1 demonstrated 93% or greater CO_2 conversion, stable performance, limited temperature rise across the reactor, and the removal of sensible heat from the circulating catalyst using a solids cooler.
- Scale-up of 100-lb batch of Cat-3 at SCI's pilot-plant facility in Louisville, KY. During bench-scale testing, it was determined that the scaled Cat-3 material possessed lower CO_2 methanation activity than the corresponding laboratory-prepared material at reaction temperatures below 350 °C.

At this time, no further development activities are planned. Further research and development activities required include:

- Increase in strength of fluidizable methanation catalyst.

  While the fluidizable Cat-1 and Cat-3 formulations possess CO_2 methanation activity equivalent or superior to commercial methanation catalysts, their strength still requires improvement. Our recommendations for improving catalyst material strength are:

  - Adding binding agents to the current fluidizable catalyst formulations
  - Increasing concentration of the support component in the catalyst formulations
  - Impregnating hardened fluidizable supports with Ni and select promoters